



High-resolution bathymetry and acoustic geophysical data from Santa Maria di Leuca Cold Water Coral province (Northern Ionian Sea—Apulian continental slope)

A. Savini*, C. Corselli

ULR CoNISM, Dipartimento di Scienze Geologiche e Geotecnologie, Milano-Bicocca University, Piazza della Scienza, 4-20126 Milano, Italy

ARTICLE INFO

Available online 29 August 2009

Keywords:

Cold-water corals
Santa Maria di Leuca
Seafloor mapping
Coral mounds
Seafloor morphologies
Acoustic facies

ABSTRACT

A total of 800 km² of multibeam echo-sounder coverage, roughly 800 km of chirp-sonar data and 18 km of side-scan sonar profiles (100/500 kHz) were acquired a few km offshore Santa Maria di Leuca (south-eastern Italy), from 200 m to 1300 m water depth. The explored area belongs to the upper slope of the gently south-eastward dipping Apulian continental margin (northern Ionian Sea). Acoustic datasets were collected, by three different oceanographic expeditions, where evidence of living cold-water coral (CWC) colonies were documented by previous surveys and samples.

High-resolution multibeam bathymetry indicated an extensive rough seafloor with an irregular faulted upper surface to the west (reflecting large-scale tectonic control on the margin) and a highly disrupted upper slope formed by prominent downslope mass-movements to the north. A broad area in the east was influenced by mass-transport deposition, which resulted in a very complex hummocky seafloor, mainly shaped by detached block-like features and failure-related bedforms (i.e. low scarps, downslope lineations and compressional ridges). From the shallow seismic-stratigraphic data, failure events appeared to be multiple and recurrent and chaotic reflectors, both buried and exposed at the seafloor, affected most of the investigated area. Drift sedimentation was also recognised along a central large ridge, resulting in an interplay between contour currents and downslope turbidity currents.

The spatial distribution of the CWC reefs was inferred from the acoustic facies interpretation based on video images and ground-truthed by sediment samples. It appeared that: (1) within the investigated area, living coral frameworks were located along large topographic highs facing the main flow of the bottom currents, where hard and firm substrata and/or failure-related sediment bedforms occurred; (2) CWC mainly settled on clustered (and isolated) mound-like features, tens to a few hundreds of metres long and no more than 25 m high and were located between 600 and 900 m water depth, within the broad area affected by downslope mass-transport deposits. Such mound-like morphologies could thus be interpreted as a result of sediment accreted by coral growth, with the consequent sediment trapping on small-scale positive seafloor irregularities; formed by different types of Pleistocene-exposed mass-transport deposits, their burial prevented by bottom currents.

© 2009 Elsevier Ltd. All rights reserved.

1. Introduction

The southern Apulian margin (northern Ionian Sea—Fig. 1) recently gained interest with the discovery in 2000 of a healthy, living, Cold Water Coral (CWC) province, a few miles off Santa Maria di Leuca (SML) (Tursi et al., 2004). The SML CWC province has since become a focus of significant research efforts: several national and international oceanographic expeditions from different research programs and activities (e.g. the 2002 CNR COR2

project, the 2003–2005 Italian APLABES project, and cooperation between the Euromargins/Eurocore ‘Moundforce’ ESF program and the EU ‘Hermes’ provided by the CNR CORSARO cruise in 2006) were initiated after the province’s discovery. Following a first attempt to locate and sample SML coral frameworks during the COR2 cruise, aboard CNR R/V *Urania* (Taviani et al., 2005a), a large-scale multidisciplinary investigation of the SML CWC province, performed during three different cruises of the Italian R/V *Universitatis* within the Italian program APLABES, provided a comprehensive geophysical survey. The main dataset, which is presented and discussed, included multibeam bathymetric data, a dense network of chirp-sonar profiles, and side-scan sonar mosaics on selected areas.

* Corresponding author. Tel.: +39 02 64482079; fax: +39 02 64482073.
E-mail address: alessandra.savini@unimib.it (A. Savini).

CWC (i.e. scleractinian azooxanthellate framework corals) were found along the ocean margins (Freiwald et al., 2004; Roberts et al., 2006; Roberts et al., 2009) as well as on seamounts and mid-oceanic ridges (Mortensen et al., 2008), and occurred on the seafloor as individual corals, isolated colonies and small to large patchy or densely distributed reefs that usually settled on and/or form mound-like features on the seafloor and sometimes develop into prominent positive morphologies called giant carbonate mounds (Freiwald et al., 2004; Roberts et al., 2009). Their widespread occurrence, forming small- to large-scale reefs and/or mound-like structures on Northern and Eastern Atlantic continental margins, has been the subject of numerous studies from various disciplines (biology and microbiology, hydrocarbon geology, paleontology, sedimentology and geophysics), the results of which have shown that the interplay between local hydrography and sedimentary dynamics is an important control factor in reef development (Freiwald, 2002; Kenyon et al., 2003; Huvene et al., 2005; De Mol et al., 2007; Wheeler et al., 2007; White et al., 2007; Foubert et al., 2008; Sánchez et al., 2008). In such ‘provinces’ where CWCs tend to cluster, proper hard substrates (allowing for the initial settlement of coral larvae), nutrient-enriched water masses (supplying food for coral growth), and strong bottom currents (keeping polyps free from sediments), often topographically driven, are the main environmental patterns constantly associated with CWC seafloor distributions (Freiwald et al., 2004).

The presence of living CWC in the Mediterranean Sea was only documented in the last decade. The use of acoustic survey techniques and remotely operated vehicles (ROVs) revealed their presence in the Alboran Sea, the Straits of Gibraltar, the Sicily Channel, the Ionian Sea, and the Southern Adriatic Sea (De Mol et al., 2005; Taviani et al., 2005a; Corselli et al., 2006; Freiwald and Shipboard Party, 2007; Trincardi et al., 2007; Schembri et al., 2007; Freiwald et al., 2009). Study of the sedimentary environment has important scientific impacts since CWC reef and mound development reflect environmental changes over geologic time scales corresponding with recurrent glacial cycles (Dorschel et al., 2005; Roberts et al., 2006). In northern Europe, stratigraphic studies from giant carbonate mounds off Ireland showed pronounced depositional cycles of coral-rich and hemipelagic sedimentation associated with glacial–interglacial periods extending back to at least the early Pleistocene (Henriet et al., 2005; Williams et al., 2006). In the Mediterranean Basin, U/Th dating suggests continuous cold-water coral growth over the last 50,000 years (Schroder-Ritzrau et al., 2003), but the temporal and spatial distributions and associated fauna diversification, as well as related paleoceanographic conditions and sedimentary dynamics, are still poorly known and thus far have received little attention (Corselli, 2001; Taviani et al., 2005b).

As documented, the SML CWC province hosts living coral colonies of *Madrepora oculata* and *Lophelia pertusa* (Tursi et al., 2004; Taviani et al., 2005a; Rosso and Vertino, 2010; Mastrototaro et al., 2010; Vertino et al., 2010), occurring as isolated colonies and as small, patchy distributed reefs (Savini et al., 2004; Corselli et al., 2006; Taviani et al., 2005a). By comparison with modern Eastern Atlantic and Pleistocene Mediterranean counterparts, modern coral frameworks display lesser-diversified associated invertebrate fauna. Evidence of strong bottom-current-related seafloor features (such as sediment drifts and seafloor erosion) documented by previous investigations (Taviani et al., 2005a) have suggested that their growth is stimulated primarily by oceanographic currents.

Interpretation of acoustic geophysical datasets collected in the framework of the National Italian project Aplabes, are presented here. We attempted to map the distribution of SML coral frameworks on the basis of their acoustic signature, as described

where ground-truth controls through video images were present (Etiope et al., 2010; Vertino et al., 2010). Seafloor morphologies and related acoustic facies were determined in order to interpret the most prominent sedimentary processes that were active in recent times in the southern Apulian margin and their possible interactions with CWC distribution and growth.

This paper should be considered as a baseline study of marine geomorphology for the uppermost part of the succession on the Apulian swell, indicating that the physiographic settings and consequent bottom-current interactions have been important factors in controlling CWC distribution along the slope.

2. Study area

2.1. Geological setting

The study area was located 9 km south of Santa Maria di Leuca (south-eastern Italy) at the southern prolongation of the Apulian peninsula into the Ionian Sea (Fig. 1), in the form of an NW–SE elongated structural high called the “Apulian swell” (sensu Auroux et al., 1985). The Apulian swell extends from Apulia to offshore from Greece and is formed by a 100-km-wide (Calcagnile and Panza, 1981) buckling anticline of continental crust. The swell separates the southern Adriatic Basin at the southern edge of the Otranto channel from the deeper Ionian Sea along the Taranto trench, and is part of the present foreland system of both the Apennine to the west and the Hellenic Arc to the east (Fig. 1). According to Gueguen et al. (1998) the foreland system can be dated to at least the Oligocene (Moretti and Royden 1988; Argnani et al., 1993), even if the roll-back of the subduction hinge (Malinverno and Ryan, 1986) slowed during the late Pliocene–Pleistocene at the front of the southern Apennines, when the accretionary wedge reached the thick continental Apulian swell in the foreland (Doglioni et al., 1994).

As shown in Fig. 1, the southern Apulian margin has a relatively narrow shelf (15 km wide); the shelf break occurs at 120 m water depth. At 200 m a marked step of roughly 300 m leads to the upper margin that showed a different morphological trend from west to east. In the northwest, the seafloor slopes down to the Taranto trench at depths of 2400 m. Here a relatively steep escarpment, of 3–5° creates a typical step-like profile, shaped by NW–SE-oriented scarps and ridges that reflect the orientation of the main extensional faults of the Apulian margin (Merlini et al., 2000; Argnani et al., 2001). The escarpment steepens towards the SW edge of the Apulian carbonate platform margin, where a sub-vertical and sinuous wall, almost 1500 m high, firmly outlines the swell that reaches more than 3500 m, bounding the Ionian Basin. To the southeast, the Apulian margin gradually deepens to 3000 m within 220 km from the shelf break, forming a rough plateau. Eastward the escarpment is gentle and reaches no more than 1200 m in depth within 40 km, facing the steep Greek-Albanian escarpment along the Hellenic arc.

The Apulian antiformal is segmented by NW–SE-strike extensional faults (with interval of about 1–2 km—Merlini et al., 2000) forming down-faulted blocks both southwestward and north-eastward, for a total throw of about 1 km (Billi and Salvini, 2003). Transfer E–W faults transversally dissect the Apulian foreland, segmenting the Puglia region in three main blocks: Gargano and Murge in the north and the lowland of Salento toward the southeast. The Mattinata and Tremiti lines form the main transfer zone that transversally dissects the Apulian foreland (Salvini et al., 1999; Billi and Salvini 2000, 2001). The Gargano strike-slip belt, formed during or before the Pliocene, is still active, as demonstrated by its seismic activity (Favali et al., 1993).

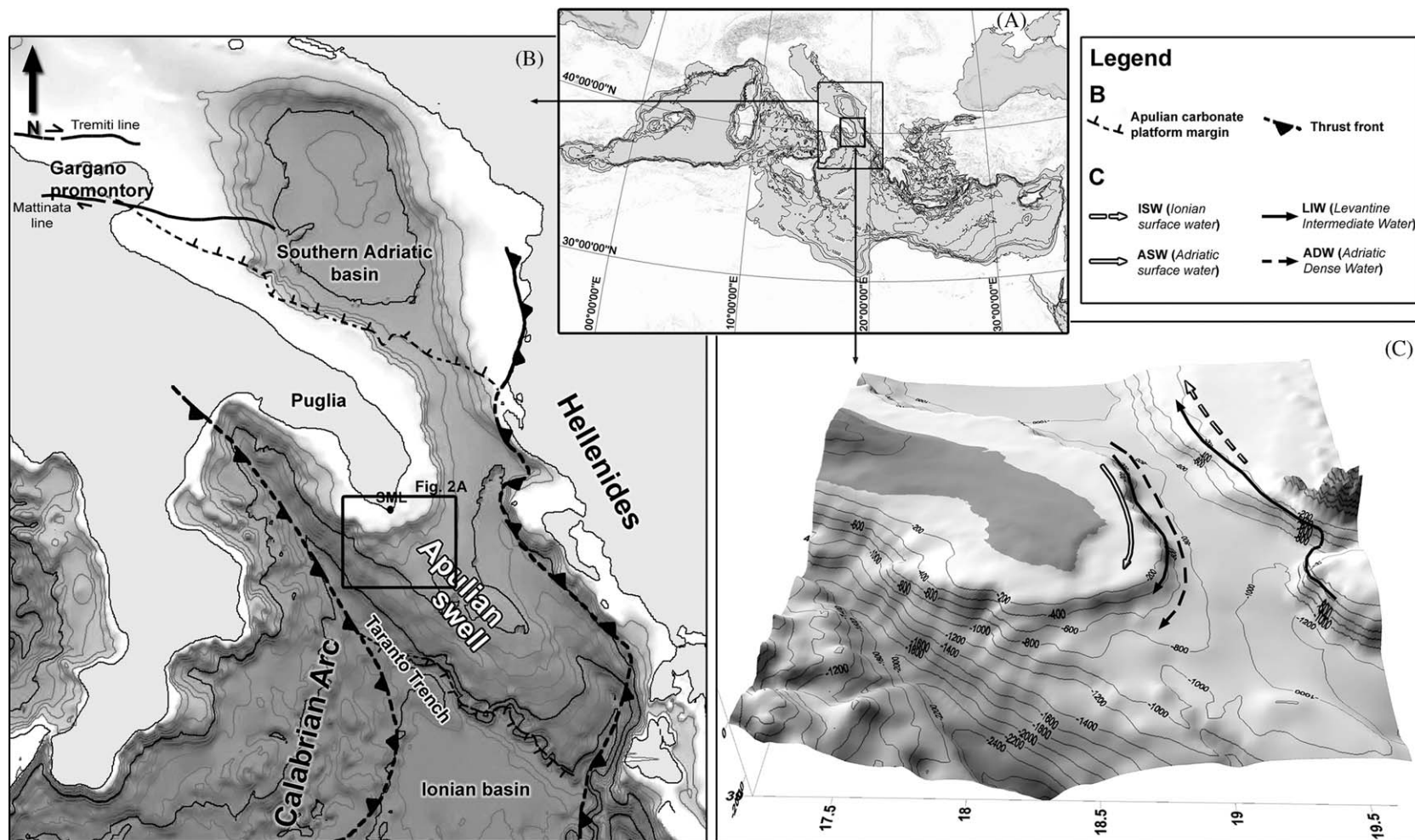


Fig. 1. Study area A: Geographical framework of the study area within the Mediterranean Sea. B: Geological setting showing the Apulian Swell as the foreland system of both the Apennines and the Hellenic fold-and-thrust belts. C: Oceanographic setting showing the ASW (Adriatic Surface Water), the LIW (Levantine Intermediate Water), and the ADW (Adriatic Deep Water) in the study area.

The Variscan crystalline basement of the Apulian foreland is overlain by a thick (6 km) Mesozoic sedimentary cover (D'Argenio, 1974). On land the outcropping of this autochthonous carbonate platform, developed on top of the Apulian swell through the Mesozoic, occurs mainly in the Gargano region and is why the Apulian foreland is often called “the Apulian carbonate platform” (Bosellini et al., 1999). Thin Tertiary sedimentary deposits are discontinuous and represented by Paleocene–Oligocene organogenic and/or calcarenous facies, overlain by thin carbonate-terrigenous deposits of Neogene and Quaternary age (Ricchetti et al., 1988). Published multichannel seismic profiles (oriented SW–NE) well mark the base of the thin Plio-quaternary sedimentary succession on the Apulian swell in the northern Ionian Sea, showing small-scale recent faults with a vertical throw between 500 and 600 m and seafloor erosional features close to fault scarps (Argani et al., 1993, 2001). A slight thickening of the Plio-Quaternary succession was observed eastward towards the Hellenic thrust front (Argnani et al., 2001).

Debates on the Apulian foreland system have dealt with several geodynamic issues mainly focused on Middle-late Pleistocene uplift and deformation of the Puglia region (Doglioni et al., 1994 and reference therein) and its seismic activity (Favali et al., 1993; Argnani et al., 2001). Indeed during the Middle-late Pleistocene the Apulian region and the Bradanic foredeep, in contrast with the central Adriatic, underwent uplift. Syn-depositional tectonic deformation, documented on-land and in the offshore area of the southern Adriatic margin (Tramutoli et al., 1984; Ridente and Trincardi, 2006), indicated that normal and transtensional faults were active during Plio-Pleistocene times, and perhaps are still active in the submerged part (Merlini et al., 2000). According to Argnani et al. (2001) active or recent normal faults on the Apulian swell may have determined the historical seismicity of the Puglia-Salento region (Camassi and Stucchi, 1996). Such faults are interpreted by the authors as a consequence of local stress accumulation due to the small curvature radius of the Adriatic Apulian plate under the double load of the Hellenides and the Appennines-Calabrian arc.

Overall sedimentation on the Adriatic margin is characterized by mass gravity-driven flows, often triggered by earthquakes (Minisini et al., 2006). Few data are available concerning sediment inputs on the northern Ionian margin of the Apulian ridge. Considering the absence of important river inputs and climate and oceanographic frameworks (see below), we would expect hemipelagic sedimentation with littoral or contour current reworking (Marani et al., 1993) and sediment transport, from the shelf on the upper slope resulting in biogenic sands by-passing the shelf break.

2.2. Oceanographic conditions

The northern Ionian Sea receives, through the Strait of Otranto, waters entering from the southern Adriatic Basin, that are the main source of Eastern Mediterranean Deep Water (EMDW) (Robinson et al., 1992). In the surface layer, colder, low-salinity Adriatic Surface Water (ASW) flows out from the Adriatic along the western side, while highly saline Ionian Surface Water (ISW) comes from the Eastern Mediterranean on the eastern side. The intermediate layer is characterised by the inflow of salty Levantine Intermediate Water (LIW) with a core at approximately 200 m depth. Adriatic Deep Water (ADW) is recognised at the bottom layer by a decrease in temperature and salinity below 600 m (Fig. 1C). Furthermore, fresher and colder Northern Adriatic Dense Water (NADW), formed in the northern Adriatic shelf during winter (Cushman-Roisin et al., 2001), flows along the western shelf (Malanotte-Rizzoli et al., 1997). The new waters

added in the northwest Ionian Basin from the Adriatic spread south and west in a near-bottom layer, entraining surrounding waters in the process and acquiring T/S properties close to EMDW (Manca et al., 2002).

Water exchange through the Strait of Otranto between the Adriatic and the Ionian Sea has been the subject of a series of experimental investigations and numerical studies. The latter have shown that climatic, hydrologic and meteorological conditions in terms of air–sea interactions and fresh-water discharges to the Ionian and Adriatic Basins on each side of the strait greatly influence variations in both the characteristics of the water masses and their dynamics. The circulation regime varies seasonally and inter-annually in response to changes in heating and wind regimes (Cushman-Roisin et al., 2001). Also geometric properties in the Strait of Otranto (minimum width of 75 km, longitudinal axis oriented almost north–south, and with a sill depth of about 800 m, separating the 1200-m-deep Southern Adriatic from the much deeper Ionian Sea) influences the dynamics of the water exchange.

The identified distribution of particulate matter in the water column south of the Strait lead to the recognition of a layered structure, where under the ASW and the LIW a bottom nepheloid layer has been identified, the extent of which varied in relation to the flow of dense bottom water of Adriatic origin with a sediment supply from the shelf area (De Lazzari et al., 1999). The nepheloid layer occurred in the bottom layer over the Italian continental shelf and in the upper slope down to 500 m, resulting in relatively high particulate matter concentrations near the bottom. A relative enrichment in particulate matter was maintained southward even at the bottom of the Ionian Basin (Boldrin et al., 2002), confirming the signal of southward advection of dense waters of Adriatic origin.

Behind the Strait of Otranto the ADW outflow flowed southward and turned west (Malanotte-Rizzoli et al., 1997). It then followed isobath contours along the Italian coast between 500 and 800 m; had the form of a bottom density-driven current, occupied the deep part of the western continental slope of the strait, and was stronger from mid-March to late June (Mantziafou and Lascaratos, 2004). Bottom currents resulted in more intense than surface and intermediate flows throughout the year. In summer, when wind forcing was weaker, flow variability along the western flank of the strait was attenuated (Kovacevic et al., 1999).

Arriving in the northern Ionian Basin the ADW resulted in a core of cold ($\theta=12.92^{\circ}\text{C}$), less-saline (38.64) oxygenated water that moved in a geostrophic balance along isobaths at 500–1000 m depth (Budillon et al., 2010). During its flow toward the Ionian interior, the ADW mixed with ambient water, changing thermohaline properties and becoming EMDW or bottom water (Manca et al., 2006).

3. Methods

The dataset discussed here was collected during three cruises carried out within the framework of the APLABES project by R/V *Universitatis*, using four acoustic systems: (1) the RESON SEABAT 8160 MultiBeam Echo-Sounder (MBES); (2) the SIMRAD EA400 SingleBeam Echo-Sounder (SBES); (3) the GEOACOUSTIC CHIRP II Sub-Bottom Profiler (SBP); and (4) the KLEIN3000 Side Scan Sonar (SSS) system. Onboard the R/V *Universitatis*, the integrated system used an IXSEA OCTANS motion sensor and gyro and a Satellite Differential GPS (SDGPS). The datum was WGS84 and the UTM projection was chosen for navigation and display, fuse 34.

3.1. Equipment

- The Reson Seabat 8160 MBES operates at a frequency of 50 kHz. One hundred and twenty-six beams are transmitted from the transducers within a fan of 150° opening angle. Return values provide bathymetric depth information at angular increments of 1.2° with a vertical resolution of 1.4 cm and 20 m of footprint at 750 m water depth. MBES data were neatly recorded using the PDS2000 software at 5 Kn along closely spaced lines with track offsets of 500–1500 m, providing complete coverage of the upper margin of the Apulian swell, ranging from 250 to 1300 m water depth.
- Data from the dual-frequency (27–200 kHz) KONGSBERG-SIMRAD EA 400 single-beam echo-sounder were systematically recorded during all cruises, thus covering the entire area, at 27 kHz frequency.
- The GeoAcoustics GeoChirp II SBP system (4 × 4 transducer array) uses advanced frequency modulation (FM) and digital signal processing (DSP) techniques giving rise to optimised seabed penetration and record resolution over the 1–12 kHz frequency range. At the surface the GeoChirp Transceiver is used to control output power levels (up to 10 kW), repetition rate and output waveform (high resolution or high penetration). The data obtained from this device were systematically recorded during all expeditions at sea using the Delph Seismic Plus software, in high-resolution mode.
- In selected areas (Fig. 2), where higher resolution of seabed features was required for sediment sampling, the dual-frequency (100 and 500 kHz) Klein3000 SSS system was used (3rd cruise). Data were acquired by the SonarPro software with the VX Works TPU Operating system. A hydrodynamic depressor was used to improve survey in deep water. The SSS towfish was deployed at a constant distance from the bottom, equal to 10–20% of the operating range, settled at 300 m, and the vessel speed was not more than 3 knots. The track of the

fish was computed from the position of the ship, the length of the tow cable (between 1000 and 1500 m) and the elevation of the fish above the seafloor. The DTM provided by the MBES data acquisition was useful to drive the SSS deployment in safe conditions on the slope. SSS data were acquired within three selected areas (MS01, MS04 and MS06, Fig. 2), where visual observations, performed during the second cruise of the Aplabes project, testified the presence of living CWC at the bottom: (1) two NW–SE-oriented profiles of 2 km length were recorded on the MS01 site at about 800 m water depth, (2) a single NW–SE-oriented side-scan sonar profile of 2 km length was recorded along the eastern slope (MS04 or ‘Alantis’ site), ranging from 400 to 700 m water depth, whereas (3) the MS06 area was remotely imaged by three NW–SE-oriented profiles, 4 km long, between 500 and 700 m water depth.

3.2. Data processing

The MBES data covered an area of 800 km² with 18 main W–E-oriented track lines about 30 km in length and three NE–SW-oriented profiles 20 km in length (Fig. 2). The multibeam data cleaning and filtering were performed by PDS2000 software package, while Surfer software (Golden Software[®]) was used to provide the bathymetric maps in UTM projection (Zone 34N–WGS84). The bathymetry was plotted on a grid at a 35 m node spacing as contour plot (Fig. 3A) to display detailed bathymetric information, as slope value (Fig. 3B) and as illuminated 3D perspective view (Fig. 3C) to visualize prominent features along the investigated part of the southern Apulian margin.

SBP and SSS data processing were performed by the Triton Elics Information (TEI) suite software packages. The navigation data were plotted in GIS application (DelphMap). From the processed seismic data we exported the GeoTiff data format. The SSS data

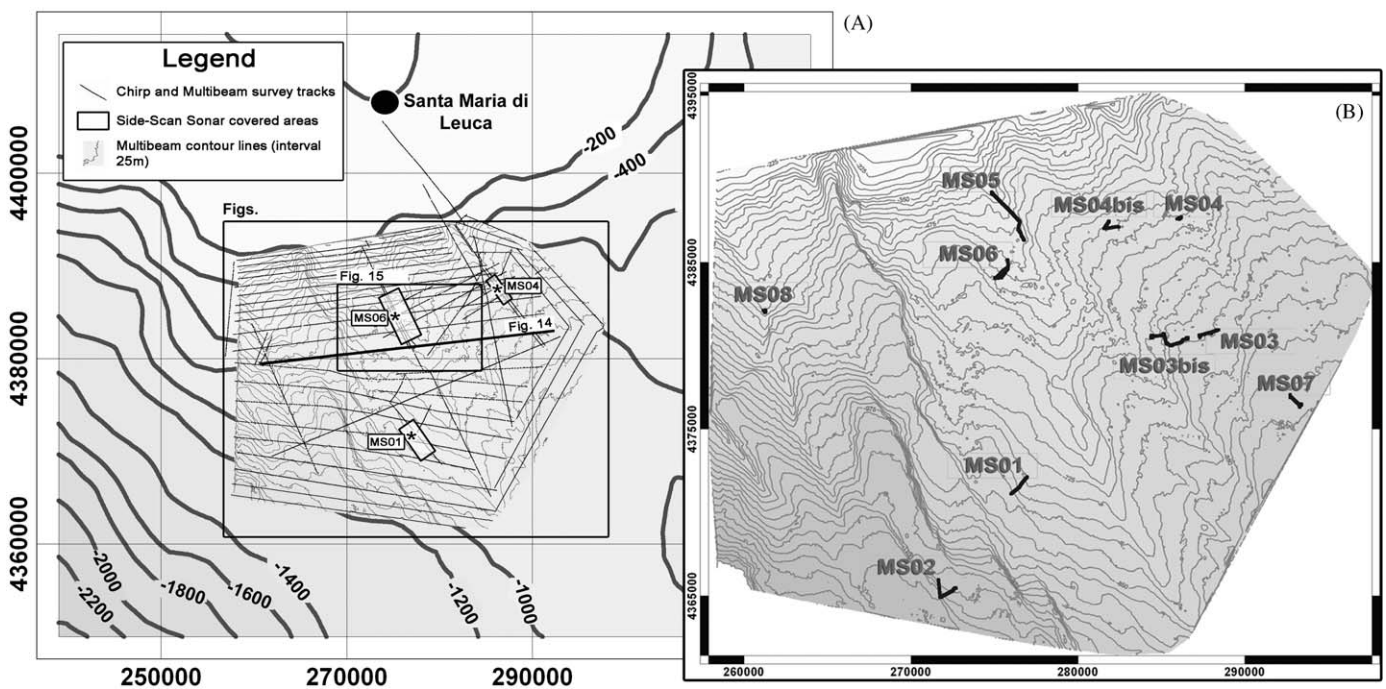


Fig. 2. A: Study area within the Southern Apulian margin. Bathymetry derived from a Reson Seabat 8160 multibeam swath sounder; contour spacing is 25 m. Multibeam and chirp-sonar survey tracks are also shown. Rectangular areas show locations of the acquired side-scan-sonar mosaics (MS01, MS06 and MS04 areas). Locations of Figs. 2B, 3, 7 and 15 and the chirp-sonar profile displayed in Figs. 14 are marked by a thick line. B: Bathymetric map of the study area (Santa Maria di Leuca Cold Water Coral province) with indication of the sites explored by the MODUS video-recording system.

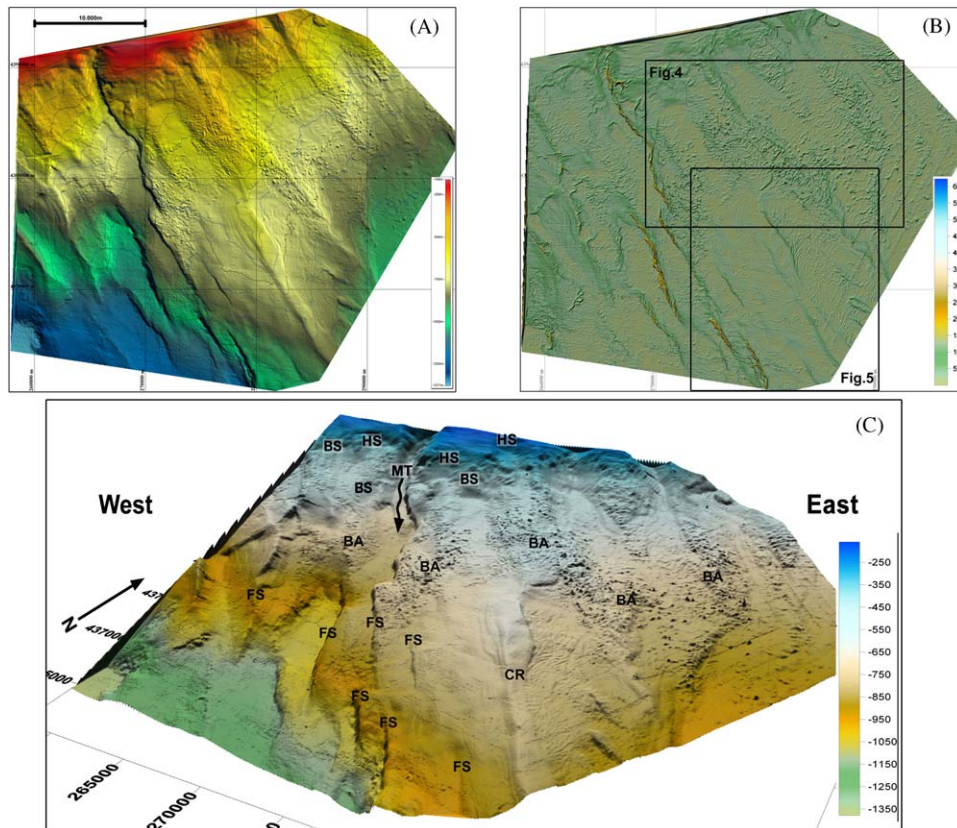


Fig. 3. Raster data provided by Reson Seabat 8160 multibeam swath sonar. A: Illuminated, color view with isobath contour lines (intervals 20 m, light from NE). B: Slope values of the study area plotted in a color view map. Locations of Figs. 4 and 5 are marked by a thick line. C: 3D view with the main identified seafloor morphologies along the investigated area (HS: Headscarps and Scarpments; BS: Faint Scarpments/buried failure scars; MT: Main Trough; FS: Fault Scarpments; CR: Central Ridge; BA: Blocky Areas).

processing provided geo-referenced grey-tone acoustic images of the seafloor at 1 m resolution.

4. Results

4.1. Bathymetry

The investigated part of the southern Apulian margin covered the upper part of the slope (close to the transition zone to the continental shelf, where the shelf break occurred at 120 m) at a depth range from 200 to 1300 m, for a total area of 800 km² (Fig. 3). The swath bathymetry map, at 35 m grid cell size resolution, showed a rough topography and a variety of seafloor morphologies, although the most prominent features observed were the NW–SE-oriented scarps and ridges, which reflected tectonic control on large-scale morphology. Fault-related scarps were more noticeable in the westernmost sector, which sloped down towards the Taranto trench, crossing distinct narrow ridges.

Northward, close to the transition zone between the continental shelf and the upper slope, a striking erosive upper slope occurred, dipping up to 4°. The bathymetric data showed several failure scars, associated transversal crack-like morphologies, and a narrow u-shaped trough (2 km wide) that indented the shelf edge. The trough cut 60–70 m into the upper slope and acted as a prevalent conduit for erosive turbidity currents. The uppermost erosive part of the slope formed for about 30 km as a rough and irregular E–W step, up to 200 m high, between 250 and 450 m

water depth. Two main arcuate steps (4 km wide on the western side and 5 km wide to the east) dissected the upper slope and several smaller escarpments (from a few hundred metres to those 3 km wide) were also widespread and often subsequently oriented in the downslope direction (Fig. 3) and documented the occurrence of repeated failures on the upper part of the margin. From 400 to 800 m depth and to the east, a hummocky topography was dominant over a gently downsloping bottom, even if NNW–SSE structural lineaments were more or less still recognisable. The rough seafloor could be associated with the eastern mass-transport zone of deposition, whose surface results dominated by mound-like morphologies, and resembled detached blocks (Figs. 3 and 4). They had irregular shapes (from elongated to less-frequent sub-circular geometries), up to 10–25 m high and 50–300 m wide along their maximum extension. Such blocky patterns were more pronounced to the east, at the top of the fault alignments oriented NNW–SSE. The identified positive morphologies were often arranged in clusters parallel to the downslope direction, creating a step-like downslope profile. Fewer blocky features were evident within the more depressed areas, where they showed a preferential arrangement along faint and sinuous small-scale sediment ridges (Fig. 4).

Beyond 600 m, a NNW–SSE-trending large-scale ridge (which we will hereafter refer to as the “central ridge”) dominated the central sector (Fig. 3) and was 5 km wide and elongated orthogonal to the margin. From deep seismic profiles, crossing the Apulian ridge from SW to NE, two reverse faults were recognised (NWN–SES oriented), isolating a wedge, extruding upward

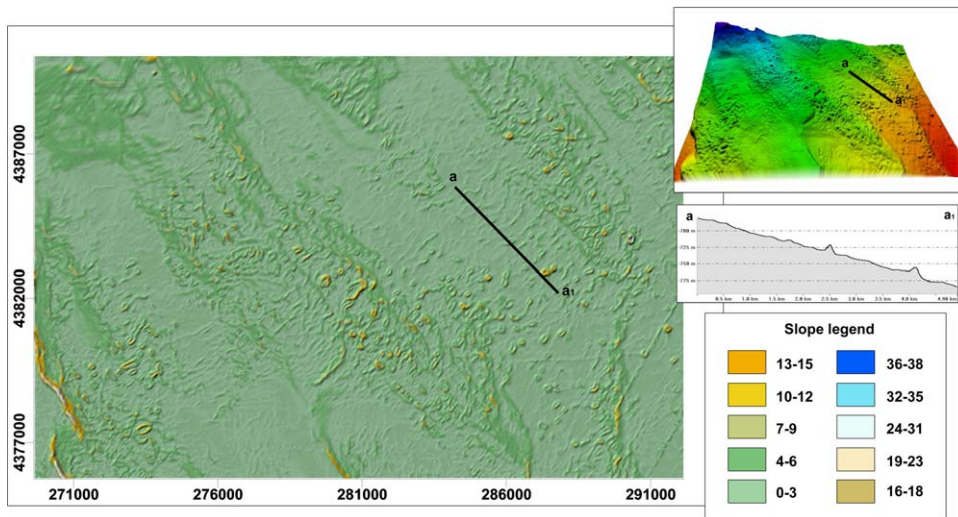


Fig. 4. Raster data provided by the Reson Seabat 8160 multibeam echosounder, shown as slope values along the main area affected by the blocky pattern. On the right a sketch of the 3D view of the same area is shown, as well as the bathymetric profile of section a-a¹, which crosses 2 blocks located within the area where they look less aggregated. Note the steepest profile downslope.

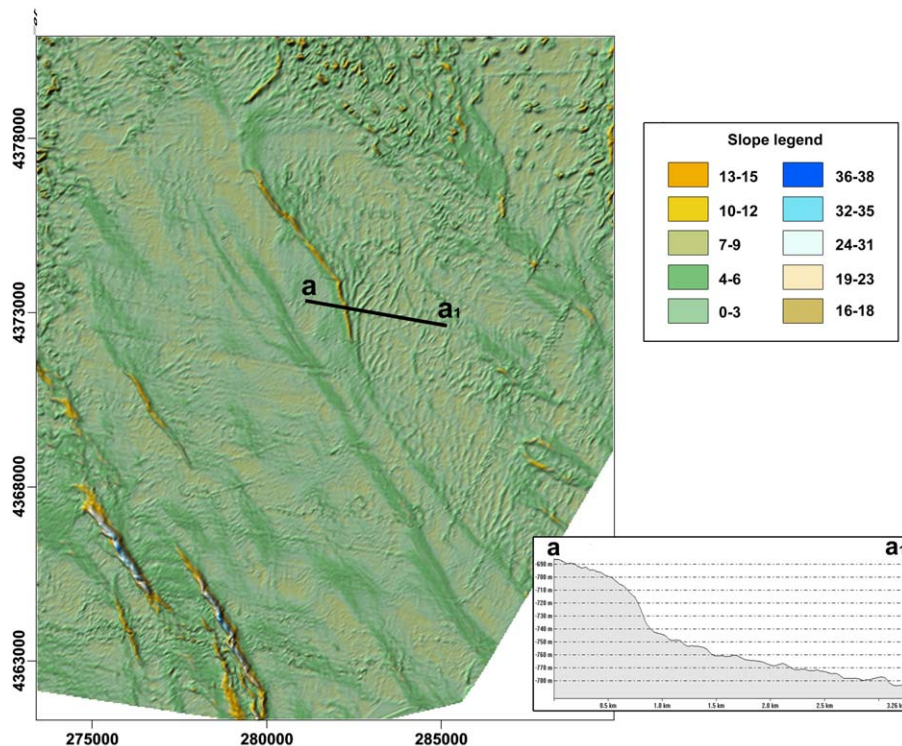


Fig. 5. Raster data provided by Reson Seabat 8160 multibeam swath echosounder, shown as slope features along the central ridge and its related failed deposits displaced at the base of its eastern flank. On the right the bathymetric profile of section a-a¹ is shown. Note the steep escarpment at the failure scar at least 20 m high and the wavy seafloor profile along the failed mass.

(Merlini et al., 2000) and forming this structural high. The crest of the ridge extended from 650 to 850 m within 16 km, separating the two morphologically contrasting western and eastern sectors and the northward failed upper slope. To the west the ridge had a nearly flat southwestward sloping surface that downsloped accompanied by a suite of fault escarpments, where the westernmost major throw reached 100 m, edging the eastern wall of the main trough that cuts the shelf break (Fig. 3). To the east, the top of the central ridge was firmly bounded by a sharp scarp, resembling a failure scar oriented NNW–SSE, up to 30 m high, that decreased in height towards the southeast. At the base of

such a failure scar, the seafloor was dominated by faint sinuous ridges (Fig. 5). They were 2–3 m high, from 100 to > 200 m wide and sub-parallel to the escarpment. In plan view they displayed a fan-shaped orientation opening towards the northeast, where they died out against the hummocky seafloor shaped by a blocky pattern (Fig. 5).

4.2. Seismic data

The main acoustic properties revealed by means of chirp profiles in the investigated area were first described by

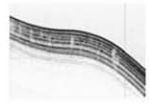
	Type	Type - example	Description	Distribution (Fig. 7)	Interpretation	Ground-truthing / References
Distinct	L_1		Strong echo surface reflector with no sub-bottom echoes. Sloping topography	Patchy-distributed along the western limbs of the north-western ridges	Outcrop of sedimentary rocks and/or firm-grounds	Sediment samples: CR41 core - it presents few cm of soft mud laying on stiff to very stiff mud up to lithified interval. The hardened sediment appears as a interval under lithification (Malinverno et al., 2010)
	L_2		Low to moderate amplitude parallel reflectors; from 20 to 30 ms in sound penetration. Nearly flat to gently sloping topography. Embedding of small-scale lens (less than 10ms) lens of acoustically transparent material	discontinuous patches occur along the eastern limb of the ridges	Pelagic/hemipelagic sediments or mud turbidites. The small scale lens of disorganised material within the first 10 ms of sediments may document the interbedding of small blocks sourced from failure events.	(Damuth and Hayes, 1977; Damuth, 1980)
Indistinct	II_1		weakly wavy and semi-prolonged echo-surface reflector sometimes bounded below by a sharp erosional surface. Nearly flat or gently sloping topography, often channelized.	Along the axis of the main trough extended from -400m down to -1200m of w.d.. Discontinuous patches are also present along the western flank of the central ridge.	The semi-prolonged surface reflector with no or rare internal reflectors suggest dominance of silty-mud sediments and fine sand. It can be related to sand/silt turbiditic sediments sourced from the continental shelf area (when channelized) or to turbiditic vs. debris flow sourced from failure events	Sediment samples: AP28, CR43 and COR2-88cores (Malinverno et al., 2010). They consist of hemipelagic silt and frequent coarser lens of sediments (turbidites sourced from shallower depth). Abundant presence of dark-coated nodules at the tops (Malinverno et al., 2010). Visual surveys: MS01, MS02 (Etiopo et al., 2010).
Hyperbolic or wavy echoes	III_1		Hummocky chaotic low amplitude reflectors, often with cross-cutting transparent hyperboles, sometimes bounded below by eroded sedimentary layers. Strongly irregular surface showing detached block-like morphologies.	Wide areas along the upper-central slope between -300 and -800m of w.d.	Failure deposits originated northward where failure scars are widespread along the upper slope	Sediment samples: AP16 and AP20 cores. They consist of hemipelagic silt and coral fragments at different intervals. Sandy to clayey silt with high lithogenic content within the underneath part. The AP20 core likely represents the upper part of a slided block, whose sediments were plastically deformed and covered by hemipelagic sequence that includes coral rubble (Malinverno et al., 2010). Visual Surveys: MS03bis, MS04, MS06 (Etiopo et al., 2010).
	III_2		Thin drape (max 15ms) of few low distinct parallel reflectors with moderate to strong amplitudes, interrupted by high acoustically transparent hyperboles (from few to 20m in height and 50 to 200m wide) and bounded below by chaotic sub-bottom schoes.	Eastern sector, along the depth belt comprised between -500m and -700m confined upslope by the echo-type III_1.	High transparent hyperboles correspond to isolated mound-like morphologies. They could be associated failed blocks of sediments that belong to the buried part of the whole failed deposit. some of them were explored by visual investigation and showed occurrence of living and dead coral frameworks at their tops.	Visual surveys: MS03, MS07
	III_3		Nearly regular wavy indistinct reflectors, no more than 5ms high and about 100m in wavelength, and diffuse acoustic unstratified sub-bottom echo, moderate to strong in amplitude. Acoustic penetration up to 30ms.	Along the eastern flank of the central ridge, bounded upslope by a steep escarpment resembling a failure scar.	This chaotic facies, accompanied by moderate signal penetration, suggests that the deposit could be formed by disorganized mud and silt. Associated ridges at the surface resemble compressional ridges.	(Damuth and Hayes, 1977; Damuth, 1980)
Combined echoes	IV_1		Low to strong amplitude reflectors slightly deformed, narrow vertical sections of reduced reflectivity and discontinuities are present. It ranges from 20 to 30ms in sound penetration. Sharp termination downslope leading to chaotic reflectors.	Small area on the upper slope close to the transition zone to the continental shelf	Pelagic/hemipelagic sediments, where the identified discontinuities (above the headscarp of the upper slope) resemble synthetic, extensional fractures and crown cracks.	
	IV_2		15 to 40ms thick drape of parallel and wavy continuous reflectors, infilling geometry on the beneath depressions formed among acoustically transparent hyperboles and chaotic reflectors. Upslope drape thickening.	Upper slope, between -300 and -500 of w.d.	This combined echo resemble a mass movement-deposit partly or totally buried by fine grained sediments, which are organised in few marked sedimentary layers	Visual surveys: MS04bis, MS05
	IV_3		Mounded external form and converging geometry of internal reflectors at the top; erosional features downslope. The decrease in depth westward is accompanied by a progressive attenuation in acoustic penetration. The uppermost reflectors have over 30ms thick.	Along the central ridge, between -650 and -850m of w.d.	Such mound-shaped sedimentary body strongly resemble a drift deposit.	Sediment samples: GC13 core. Dominated by mud content (Fusi et al., 2006)

Fig. 6. List of the main chirp-sonar echo-types identified along the investigated area.

Fusi et al. (2006) and Taviani et al. (2005a). However, the dense grid performed by the Aplabes project allowed a better interpretation, particularly concerning the spatial distribution of the sedimentary processes affecting the southern Apulian margin. Following the scheme of Damuth and Hayes (1977) and Damuth (1980) with the support of sediment samples results (Malinverno et al., 2010) and visual surveys (Etiopie et al., 2010; Vertino et al., 2010), we recognised four main classes of echo-types along the investigated area. They are summarized in Fig. 6, while their relative abundances and distributions (along the investigated seafloor) are shown in Fig. 7.

High-resolution multibeam bathymetry combined with described chirp-sonar echo-types documented the high morphologic complexity of the study area. In particular, the investigated part of the southern Apulian margin showed clear evidence of seafloor instability, including extensive failure scars on the upper slope (Fig. 3), the broad eastern area affected by blocky slide deposits (Figs. 3 and 4), and debris on the seafloor that covered the western part of the central ridge and filled the main trough that cut the shelf break westward (Figs. 7 and 8).

Therefore overall sedimentation seemed to be dominated by mass gravity-driven flows. Mass-wasting deposition was documented by the preponderance of wavy and hyperbolic echoes in the seismic data (Figs. 6 and 7) and the lack of important areas covered by thick sequences of continuous and thin parallel reflectors, which usually documented pelagic/hemipelagic sedimentation and an undisturbed seafloor (i.e. the echo-type I-B of Damuth and Hayes, 1977). Indeed, thick acoustically transparent

deposits (echo-types III_1, III_2, III_3 and IV_2) were seen in more than 700 km² (Fig. 7) and were buried along the upper part of the slope and at the deepest depths toward E (echo-type IV_2), while they occurred exposed at the seafloor (echo-types III_1 and III_3) or partly buried (echo-type III_2) between 500 and 800 m (Fig. 7).

Erosional surfaces (usually characterized by high-amplitude reflectors with no sub-bottom echoes and/or diffuse returns on seismic profiles and a rough seafloor, i.e. echo-types I_1 and II_1) were more evident along the western sector of the study area (Fig. 7) and were associated with the irregularly faulted upper surface, outlined by large-scale narrow ridges (oriented NNW–SSE), whose steeper western flanks showed strong echo surface reflectors with no sub-bottom echoes and strata truncation at the top. Here the outcrop or subcrop of old consolidated sedimentary successions could be reasonably supposed (Fig. 8). The eastern gentler steeping flanks, in contrast, were mantled by reflectors (20 m thick, in some cases nearly onlapping the crests) or covered by mass-wasting deposits (Fig. 8). Slope erosion was particularly evident along the western upper side of the central ridge (Figs. 5 and 9), where a huge erosional surface extended from 600 to 900 m depth. A decrease in depth westward along the ridge was accompanied by a progressive attenuation in acoustic penetration and the occurrence of erosional truncations and small-scale incisions (Fig. 9). At the top of the central ridge the reflectors are over 30 m thick and exhibited a marked cyclic pattern of deposition represented by alternating high- and low-energy packages, nearly conformable to the seafloor. Core samples

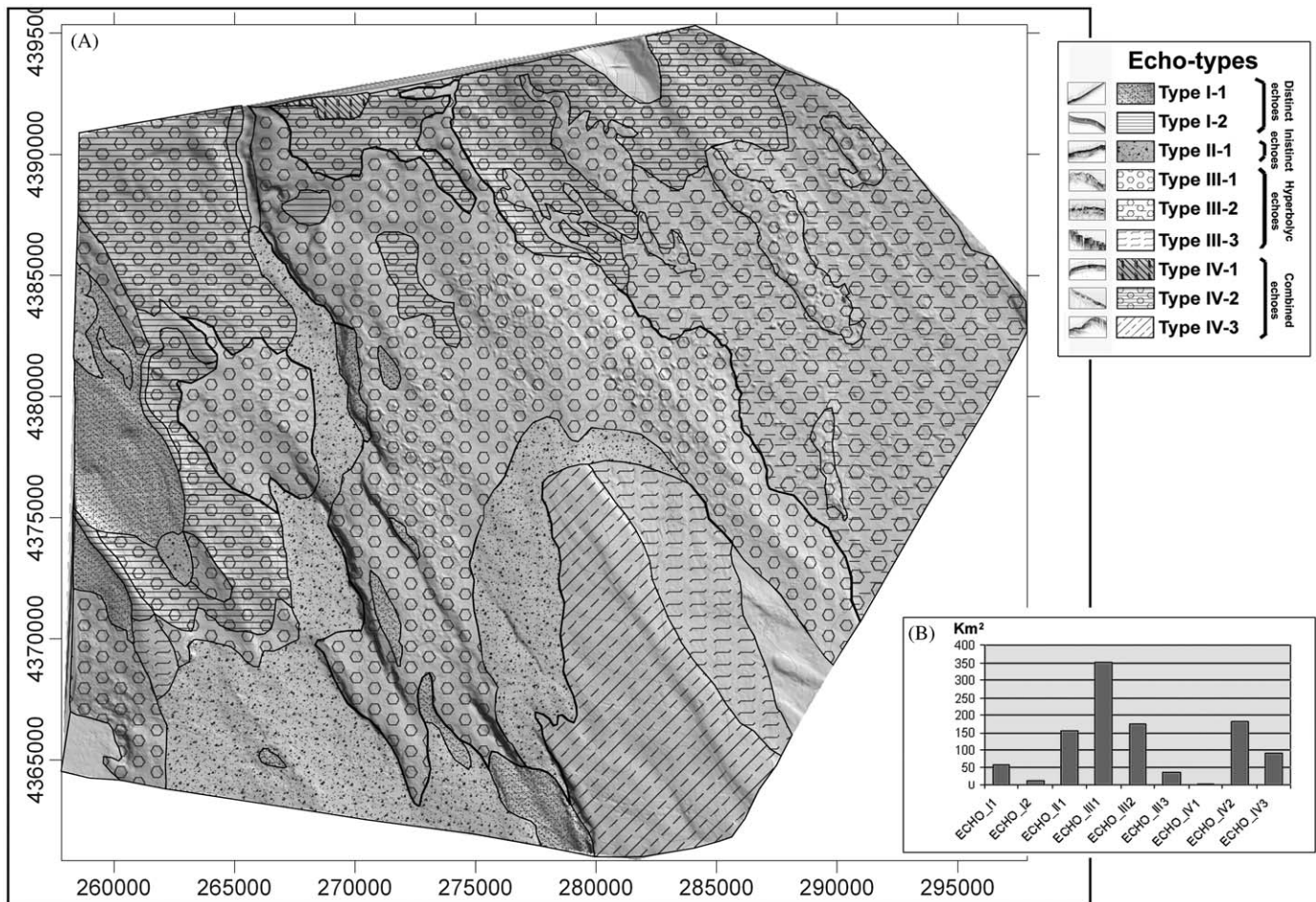


Fig. 7. A: Chirp-sonar echo type distribution along the investigated area, displayed on the acquired multibeam bathymetry (see location in Fig. 2). B: Abundances of the identified chirp-sonar echo types along the investigated area, on the base of their areal coverage.

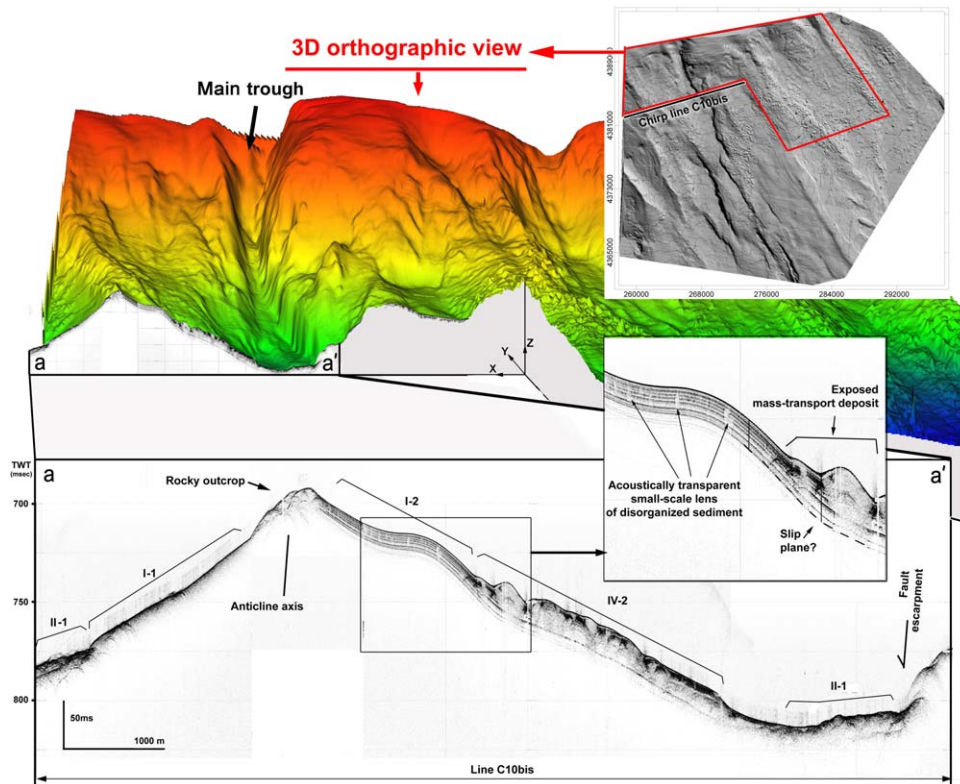


Fig. 8. 15-km-long chirp profile (C10bis line) across the western upper slope and related identified chirp-sonar echo-types.

revealed that they consisted mostly of mud (Fusi et al., 2006). The top was characterised by a mounded external form and a converging geometry of the internal reflectors, while erosional features occurred downslope (such as truncated reflectors and small-scale incisions—Fig. 9). As already suggested by Taviani et al. (2005a) such a mound-shaped sedimentary body could be related to drift deposits.

Worth noting is that erosion mostly takes place along the western side of the Apulian antiform. Here, the regional and pronounced faults, oriented NNW–SSW, showed a suite of sub-parallel scarps, creating to the SW a step-like margin profile, which abruptly sloped down to the Taranto trench, for a total throw of 2400 m in less than 50 km. To the east of the central ridge, no relevant escarpments were marked by the surface morphology. Indeed, Plio-Quaternary sedimentation slowly thickened along the eastern side of the Apulian antiform; NNW–SSE extensional faults were recognised along published deep seismic profiles (Argnani et al., 1993) and recent activity has been inferred (Merlini et al., 2000). Since mass gravity-driven deposits seem to represent the main sedimentary product within the investigated area (sourced from the upper slope), they have nearly masked the original lineaments to the East.

4.3. Side-scan sonar results

Exploration by means of 100–500 kHz Side Scan Sonar was carried out in three main zones (MS01, MS04, MS06—Fig. 2), whose previous visual investigations confirmed the presence of CWC (Etioppe et al., 2010). An exhaustive description of several SSS-identified acoustic facies is given in Vertino et al. (2010). Here we attempted to describe the relevant identified morphologies where substrate hosts CWC and their variation and dependencies with the sedimentary processes that formed them.

4.3.1. MS04 and MS06 mosaics

MS04 and MS06 sites were located within the most prominent eastern and central mass-transport deposition areas (Fig. 2), in which the blocky pattern of exposed failed material represented the most striking feature of the surface topography (Fig. 4). From video investigations, CWC frameworks were observed at the top of investigated positive seabed irregularities, formed by exposed mass-transport deposits. Living and dead colonies of deep-water corals and coral fragments were encountered on the summits and in the upper parts of several such “mound-like” morphologies (Etioppe et al., 2010; Vertino et al., 2010). The mounds hosting CWC frameworks appeared on seismic profiles as very high transparent hyperboles (Fig. 10). At MS04 and MS06 sites seismic hyperboles were imaged, in the side-scan sonar mosaics, by irregular and NNW–SSE sub-elongated positive structures (Figs. 11 and 12). They were up to 25 m high, forming important shadows on the mosaics, and 50–200 m wide along their maximum extension. As shown in Figs. 11 and 12, the seafloor within this area was very irregular. Different types of backscattering (from low to very high) were recognised. Mound-like shapes ranged from sub-circular to narrow and elongated seabed features. They ran sub-parallel to the isobaths and were aligned perpendicular to the slope. The most characteristic acoustic features, defined by different acoustic backscattering and the surface morphologies were as follows:

- High to moderate backscattering pattern diffuse at the top and along the eastern side of the positive seabed structures, associated with the mound-like morphologies recognised on the multibeam map. Corals were mostly settled on the northeastern flank and at the top of distinct topographic features (Vertino et al., 2010), in association with the distinct backscattering pattern (Fig. 11).
- The widespread clusters of close-set stripes of moderate backscattering found within the MS06 mosaic (Fig. 12):

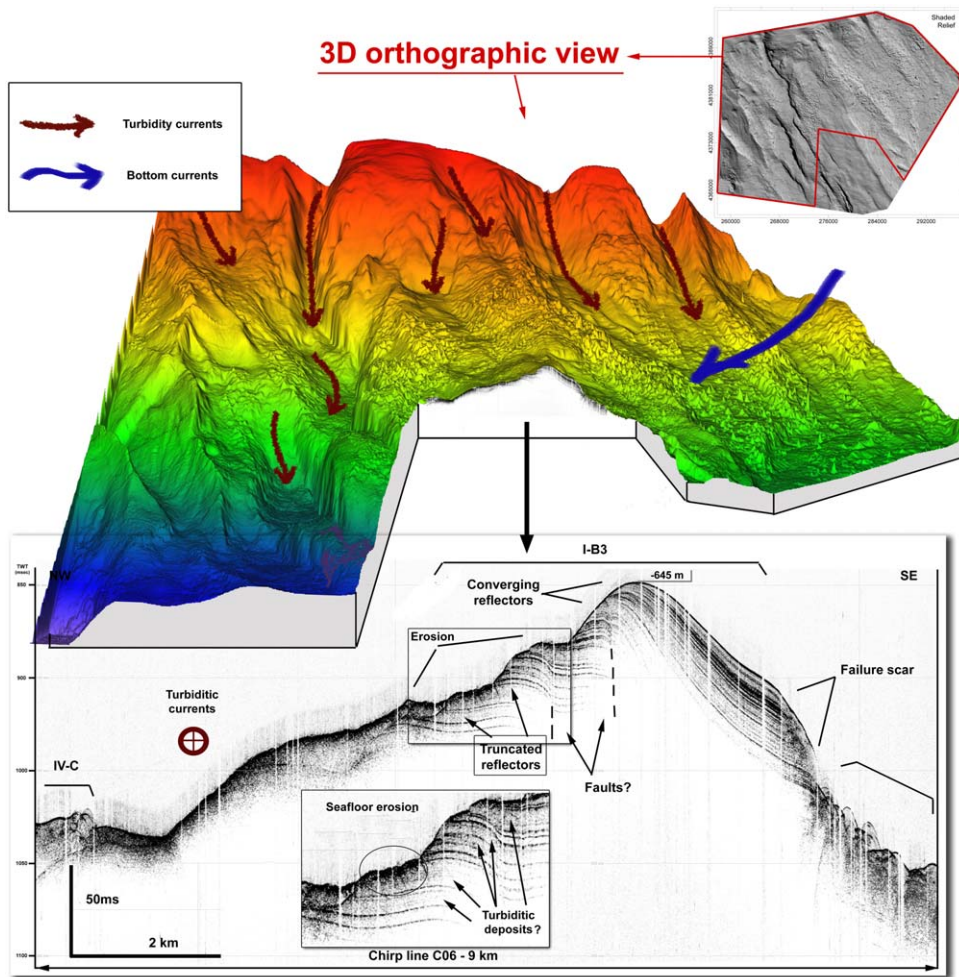


Fig. 9. 12-km-long chirp profile (C06 line) across the central ridge and related identified chirp-sonar echo-types and sedimentary features.

interpreted as small-scale sediment ridges, resembling extensional features within the mass-transport depositional area that mostly occurred along the dipping side of the downslope step-like profile of the mass-transport deposit (Fig. 12).

- Areas of moderate to quite strong grey tones, associated with a high percentage of sand and gravel at the surface (i.e., coral rubble, Vertino et al., 2010) that mainly occurred close to the top of several mapped mound-like morphologies along their western flanks (Figs. 11 and 12).
- Elongated and distinct lines of high backscattering on the western side of positive seabed irregularities (Figs. 11 and 12) that can be associated with small-scale steps causing a bigger angle of incidence and to (as visually observed on video data) that are evidence of hard-substrata occurrences (i.e., strata truncation and exhumation of older lithologies due to failure).

4.3.2. MS01 mosaic

The MS01 site has been investigated by two single side-scan sonar profiles crossing the chirp-sonar facies II-1 in the NNW–SSE direction along the western part of the central ridge (Fig. 2). The mosaic covers a nearly flat area, where debris vs. turbiditic deposits, subject to erosion and reworking, define the present-day sedimentary environment (Malinverno et al., 2010). Indeed from Fig. 13 the seafloor appears to represent an area of widespread seafloor erosion. A predominant moderate to strong backscattering dominates the obtained side-scan sonar mosaic with

a complex acoustic fabric. Small-scale seafloor irregularities with up to 3 m of relief were also evident (Fig. 13). The most characteristic acoustic features were as follows:

- Dark and highly contrasted backscattering patterns that were widespread in the central part of the covered area, and that seemed to follow their distribution in a prevalent N–S direction in different shapes (from elongated to less-frequent sub-circular geometries). As we can infer from geophysical data, the complex sedimentological fabric of the area (impacted by multiple debris and turbidity flow deposits) resulted in a rather rough topography characterized by random relief not higher than 3 m with a hint of an aligned spatial arrangement in the downslope direction. According to the acoustic facies on the side-scan sonar mosaic, they seem to be erosional remnants, and they appeared on the related chirp-sonar echo-type as small-scale transparent hyperboles (Fig. 13A and C). According to visual observations (Etioppe et al., 2010) and sediment data (Rosso and Vertino, 2010; Malinverno et al., 2010), small CWC frameworks, formed by both living and dead colonies, were often associated with such acoustic facies, where high backscattering was evident. Mn-coated crusts of hard-ground (Malinverno et al., 2010; Rosso and Vertino, 2010) were also recovered in these areas.
- Elongated and linear patterns, parallel to the main flow of downslope transport, were identified and resembled longitudinal

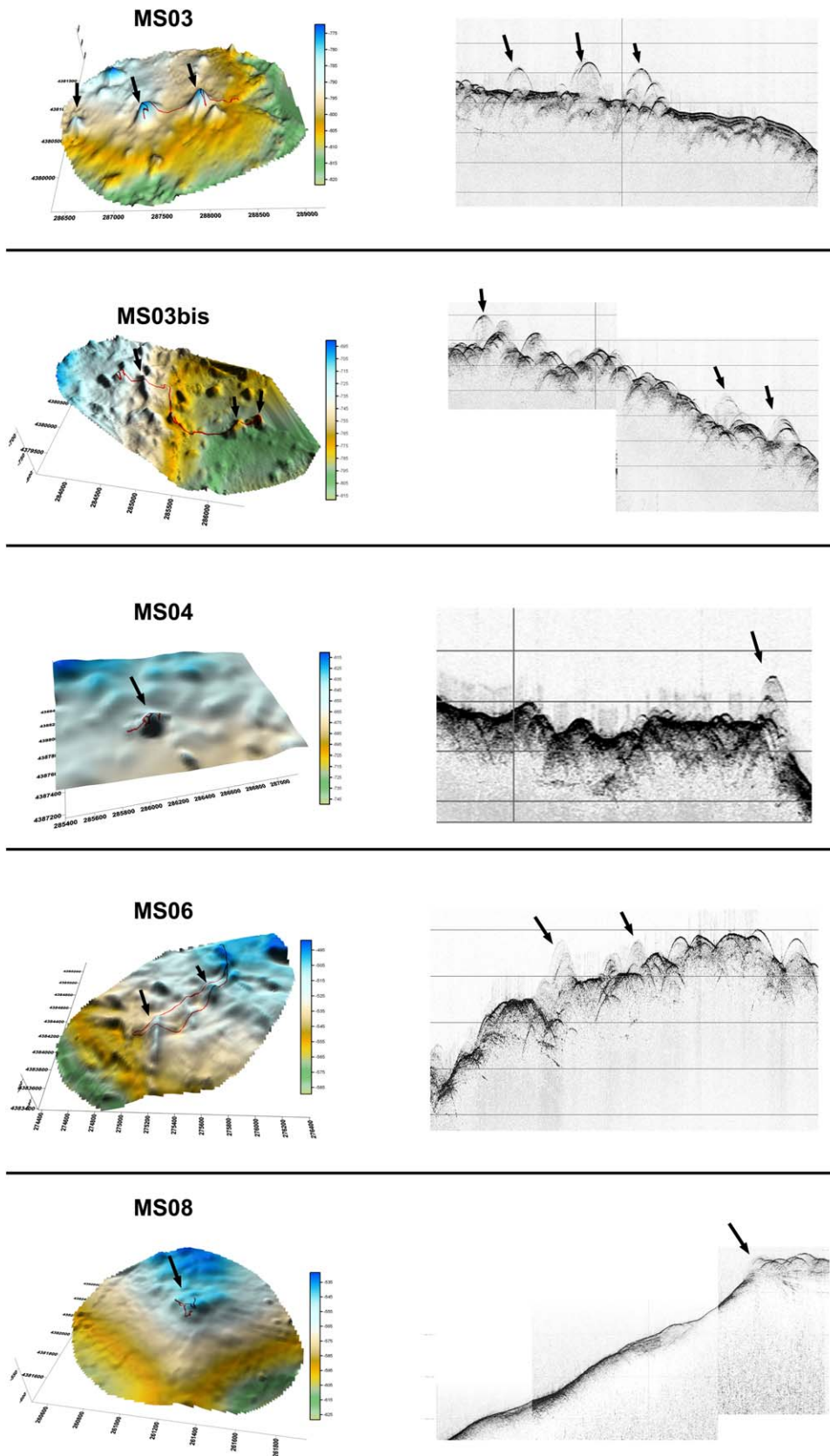


Fig. 10. Examples of the detailed multibeam bathymetry and chirp-sonar data collected along the visually explored areas where the CWC were found (see Fig. 2 for location of the sites explored by the MODUS video-recording system). Arrows indicate correspondences between multibeam and chirp-sonar data at the sites where living and dead coral colonies have been visually detected.

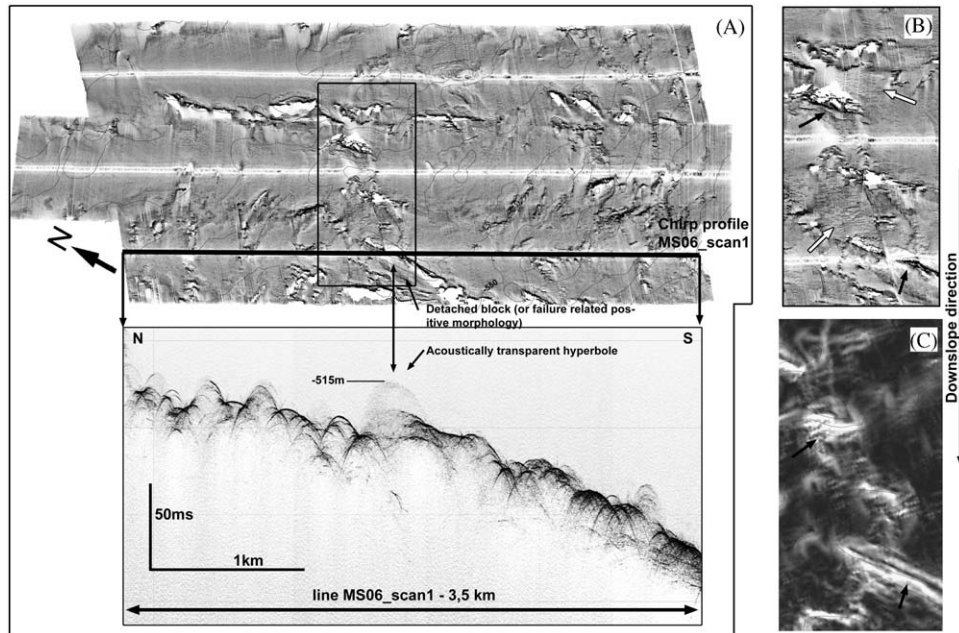


Fig. 11. A: Side-scan-sonar mosaic and chirp-sonar seismogram sections from the MS06 site. B: Side-scan sonar detail (locations in (A) marked by a thick line); white arrows indicate cluster of parallel close-set stripes interpreted as sediment ridges; black arrows indicate the steepest western profile across single positive relief hosting coral frameworks, showing the down-dip termination of the blocky pattern (see Section 4.3.1 for description). C: Slope image of the same section shown in B.

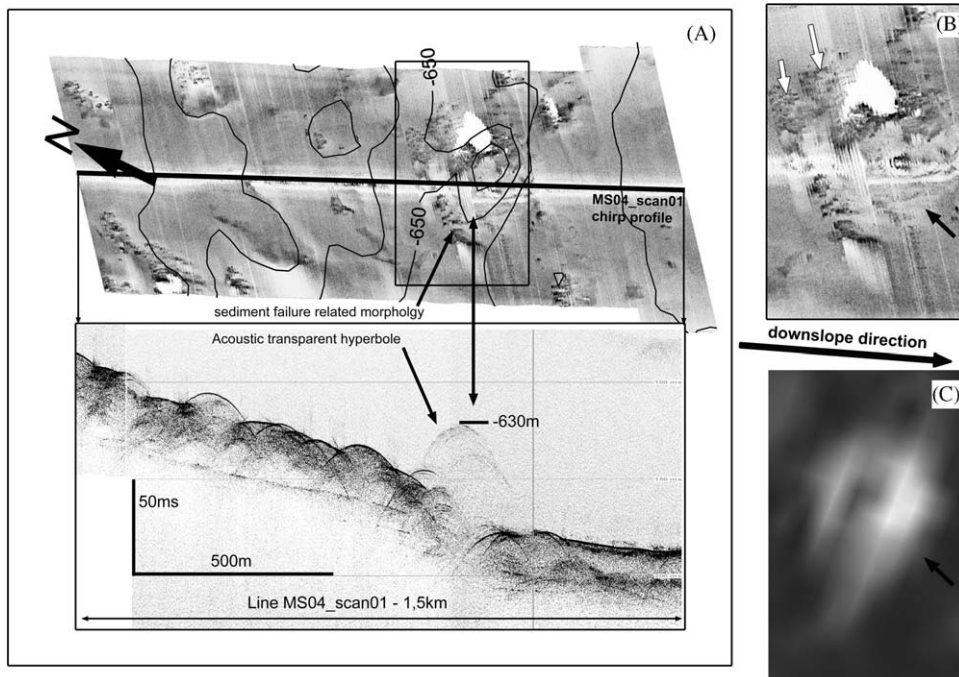


Fig. 12. Side-scan sonar images and chirp-sonar seismogram sections from the MS04 site. B: Side-scan sonar detail (locations in (A) marked by a thick line); white arrows indicate a cluster of highly contrasted medium to high backscattering patterns where CWC occur; black arrows indicate the steepest south profile across the single investigated positive relief hosting coral frameworks (see Section 4.3.1 for description). C: Slope image of the same section shown in B.

boundary shears marking the edges of more fluidified material across a rather hummocky topography (Fig. 13D).

- Widespread seafloor marks, resembling scours, and erosional lineations were also evident (Fig. 13B).

The highly variable backscattering shown by the mosaic was interpreted as being a mixture of sediment erosion and deposition. CWC were found in areas where erosional remnants,

consisting of firm- to hard-ground substrates, were suitable for their settling and growing.

4.4. CWC acoustic facies distribution

Observing the main locations in which CWC were sampled or visually documented, the occurrence appeared to be strictly

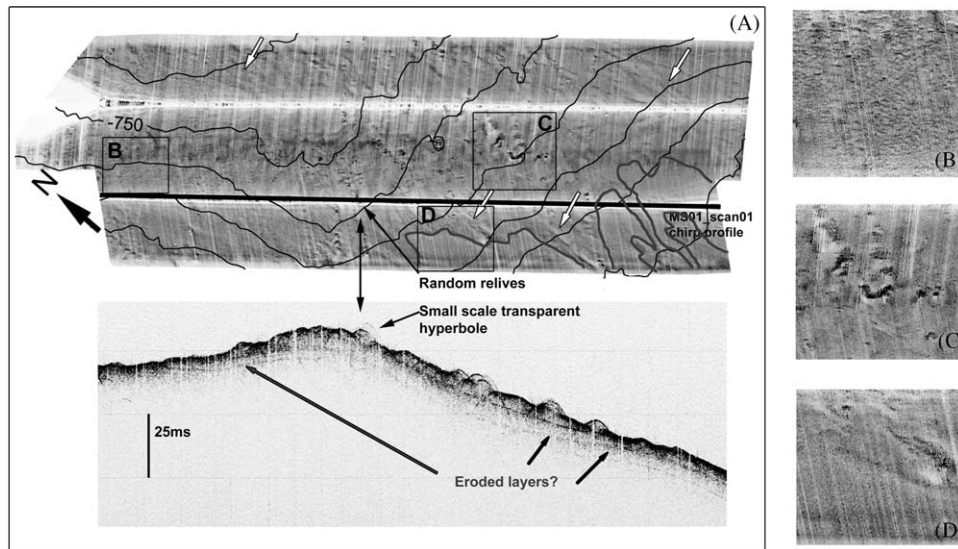


Fig. 13. Side-scan sonar images and chirp-sonar seismogram sections from the MS01 site. White arrows indicate a linear pattern. B: Side-scan sonar detail showing sub-parallel and discontinuous close-set stripes, interpreted as a complex zone of scours; C: Side-scan sonar detail where high backscattering patterns are identified associated with small-scale relief. D: Side-scan sonar detail showing rather undisturbed sediment and the downsloping lineation marking a lobe of disturbed sediment probably associated with debris vs. turbidite deposits.

associated with acoustic anomalies, resulting in very high acoustically transparent reflection hyperboles on chirp-sonar profiles (Fig. 10). Where the seafloor hosts living or dead coral frameworks, the intensity of the reflected echo, recorded both from the chirp-sonar and the single-beam echo-sounder, is significantly lower than that of surrounding sediments, meaning that part of the energy has been absorbed or reflected elsewhere. Such observations have led to the selection of sites at which the first visual observations on the SML CWC province were performed (Etioppe et al., 2010). Ground truth controls by video surveys also confirmed this relationship in sites where CWC have not yet been documented by sediment samples.

Since among the first hypotheses explaining CWC genesis and growth, the “seepage hypothesis” (Hovland and Thomsen, 1997) linked the occurrence of carbonate mound hosting living CWC to the seepage of light hydrocarbons, such an acoustic pattern was initially associated with the possible occurrence of gas-charged sediment resulting in wipe-out zone and/or acoustic turbidity on chirp profiles; these signatures are often considered diagnostic for the presence of gas within sediment (see Sager et al., 1999 and reference therein). Methane sensor observations revealed that sediments are not fluid-bearing, indicating that the development of the coral colonies is not linked to seeping fluids (Etioppe et al., 2010).

Based on video observations, obtained seafloor morphologies and high-resolution seismic data, three main geomorphological settings can be identified in which CWCs occur:

- The main echo-types encompassing high acoustically transparent reflection hyperboles (where CWC were visually observed at their tops) were typical of more or less chaotic mixtures of sediments emplaced by large-scale downslope mass-movements (echo-types III_1, III_2), as already pointed out by Taviani et al. (2005a). The main seafloor morphologies hosting CWC were thus identified within the most prominent mass-movements and mass-transport deposition areas (Figs. 7, 11 and 12), which place on more than 600 km², between 600 and 900 m in water depth.
- Isolated and patchy distributed colonies were also found along the western flank of the central ridge (Fig. 13), within an area

densely affected by erosion and reworking driven by debris vs. turbidite flows and where ferromanganese hardgrounds occur (Malinverno et al., 2010; Rosso and Vertino, 2010), likely growing on erosional surfaces due to bottom currents.

- Along the western side of the investigated part of the Apulian antiform, CWC were visually documented at the top of fault escarpments where the outcropping of hard substrata had been inferred (Figs. 8 and 10).

5. Discussion

5.1. The upper slope and mass-wasting-dominated areas

The identification of displaced sediments along the investigated area was aided by irregular morphologies, and the associated occurrence of chaotic ecotypes (III_1, III_2, III_3 and IV_2), and parabolic features, the latter possibly due to more coherent blocks of material within the disaggregated mass. Failed deposits resulting in a hyperbolic surface echo without sub-bottom echoes occurred either exposed at the seafloor (echo-types III_1 and III_2) or buried below a draped sedimentary unit (echo-type IV_2). Where the deposits were not buried or were buried by a thin drape of sediment, resulting surface-positive morphologies mostly occurred as isolated or as clusters with small-scale positive relief had sub-circular to elongated shapes, and were interpreted as a blocky pattern of mass-transport deposits (Fig. 4). Some of the blocks measured more than 500 m in diameter (along their major axis), while the average size was 200 m. They rose from the seafloor up to a 25 m maximum. The failed deposits have, for the most part, a locally erosional base and a hummocky top shaped by a blocky pattern, both indicative of deposition through mass-transport processes. Heavily deformed sediments and blocky patterns dominated the eastern sector, extending over more than 600 km² (Fig. 7) for more than 15 km downslope at a low angle (1.1°). The occurrence of large arcuate headscarps indenting the shelf break (Fig. 3) and extensive deposits of blocky, acoustically transparent debris, transported considerable distances over very low angles, suggest the dominance of resedimentation processes along the upper part

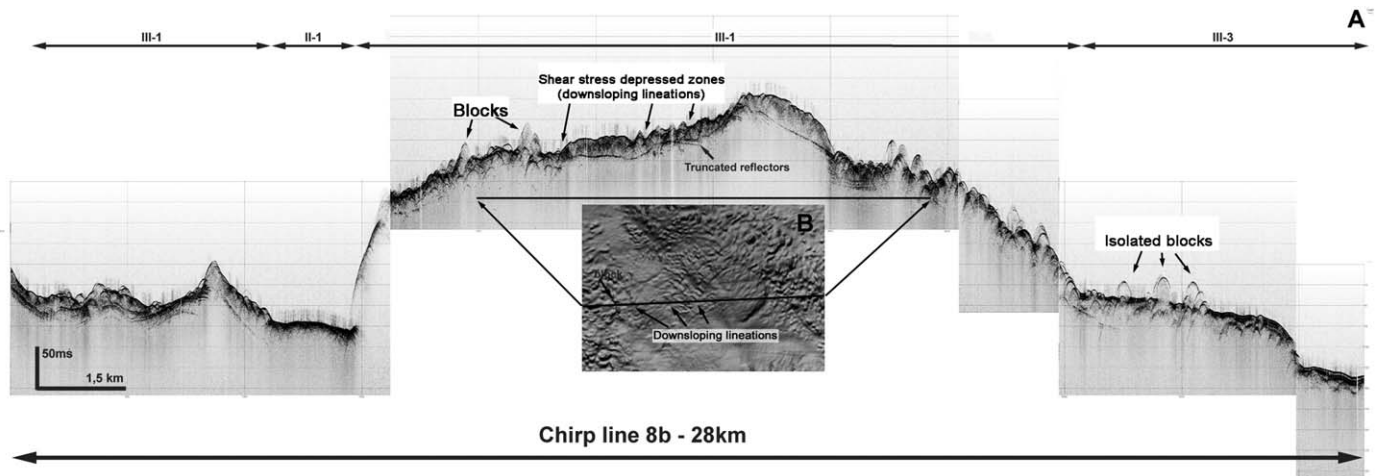


Fig. 14. 28-km-long chirp-sonar profile (C08b line) across the investigated area (see Fig. 2 for location).

of the Apulian margin, such as slides and debris avalanches (Coleman and Prior, 1988).

Following the cor8b profile (Fig. 14), crossing the study area from west to east, different deposits and related seafloor morphological expressions could be identified. On the basis of 2D seismic profiles acquired within the studied area, the character of individual deposits could not be entirely discerned. In some cases a wedge geometry and compressional features marked the toe of distinct failure events (Fig. 14), and suggested different downslope mass-transport directions, a supposition supported by a gradient slope that was tectonically defined. Indeed, the large-scale down-thrown faulted regional blocks (formed on the Apulian swell by NW–SE-oriented extensional faults—Fig. 3) outlined a prevalent southward downslope direction in the eastern sector and a southwestern direction in the west.

The edges and the prevalent alignments of the blocky pattern were defined by several negative seafloor morphologies, such as small scarps (at their downslope base) and distinct lineations (Figs. 14 and 15). The small scarps were interpreted as detachment zones among clusters or single blocks of sediment, clearly elongated where the blocks were aggregate in the downslope direction. Extensional features also appeared, in the same area, on the side-scan-sonar mosaic (extensional ridges on Fig. 12). Downslope lineations separated the failed blocks of sediments created by different mass-movements. Such a morphological configuration was often reported for slide deposits in which transverse cracks and longitudinal shear stress depressed zones occurred, respectively, as small scarps and downslope lineations (Prior et al., 1982).

Worth noting is that a prevalent block aggregation is mostly found along the large-scale topographic highs formed by regional extensional fault steps (Fig. 3), whereas within the more depressed eastern sector a large area is characterized by isolated blocks that are not as aggregated (echo-type III_2, Fig. 7). Although they did not show a prevalent alignment, they occurred at the downsloping steeper edge of small-scale wavy elongated extensional ridges (formed as gravity-driven sediments moving downslope) (Figs. 5 and 14).

5.2. The central ridge: sediment drift occurrence?

From a deep seismic profile crossing the Apulian swell from SW to NE, two reverse faults were recognised (NWN–SES-oriented), isolating an upward-extruded wedge at the top of the swell. These reverse faults seemed to affect both the Mesozoic Apulian carbonate platform and Neogene–Pleistocene sediments

(Fig. 6 of Merlini et al., 2000). Along such a structural feature, forming the NWN–SES-oriented central ridge, a NNW–SSE elongated sediment drift (Taviani et al., 2005a) with an asymmetric E–W mounded profile was recognised, at a depth range of 700–1000 m (Fig. 9) and occurred perpendicular to the slope trend following the southern Apulian margin corner along which contour currents turned from NE to SW (Budillon et al., 2010) (Fig. 1C). The axis can be followed on chirp profiles for at least 17 km, but could extend farther as there were no multibeam and chirp data beyond 1100 m depth. The elongated drift-like feature was roughly 4 km wide, gently rising from the surrounding seafloor from about 30 m westward, while to the east it showed abrupt strata truncation, resembling a failure scar (Fig. 3). According to Faugères et al. (1999) this could be interpreted as a mounded drift, developed under the influence of bottom contour currents along a margin corner (represented by the Southern Apulian margin), although we found a NE-upslope migration (Fig. 9). The upslope migration resulted in accretion on the northeastern flank of the ridge (which underwent failure eastward) and erosion along the southwestern flank. Over this western region reflectors downlapped seaward onto an erosional surface that truncated earlier sediments. Such prevailing erosion and/or non-deposition suggests the erosional influence of turbidity vs. debris-flow events (Fig. 13). The resulting drift developed under the influence of turbidity and bottom contour currents (Fig. 9). Similar configurations in sediment-drift formation were found by Rebesco et al. (1996) and explained by Faugères et al. (1999) as intercalated turbidite and contourite deposits.

Along the eastern flank of the drift a 17-km-long failure scar was recognised, documenting the failure of the top of the drift, which was interrupted eastward by a vertical escarpment of approximately 30 ms. At the base of the scar to the east a broad field of sediment ridges was recognised, resulting in chirp echo-type III_4. They reached wave lengths of 200 m and amplitudes of 5 m, and were emplaced over the drift failed deposit. Such sediment ridges may represent the resulting morphology of the slump event (i.e., slump compression waves), although the occurrence of few and discontinuous horizons (differently widespread over the chaotic deposit) may suggest bottom-current-related developments of the failed deposit.

5.3. Erosion towards the west

Merlini et al. (2000) tentatively interpreted the southwestern scarps on the Apulian plateau as an example of foreland inversion

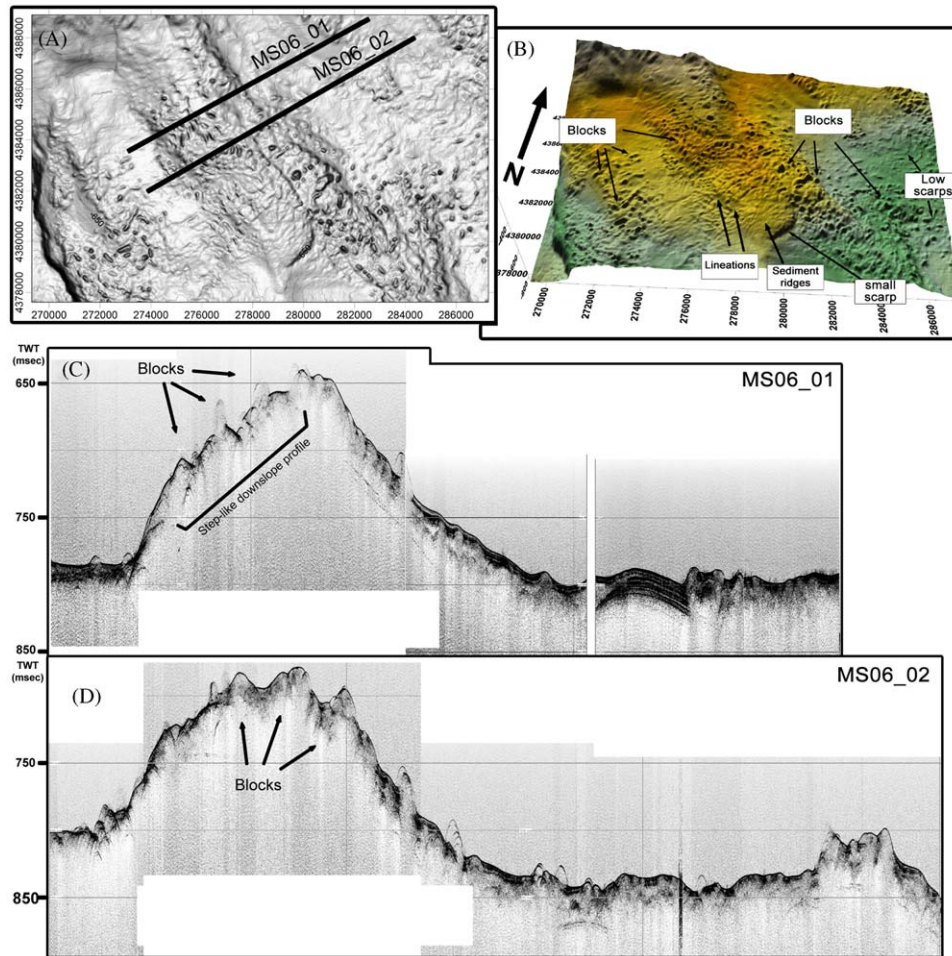


Fig. 15. Bathymetry and chirp-sonar seismogram sections along the central upper slope, where mass-transport deposition was prominent. For location see Fig. 2. A: slope image. B: 3D prospective view of the same area where some of the failure-related seafloor morphological features are indicated. C: Chirp section of the MS06_01 profile. D: Chirp section of the MS06_02 profile.

and thus hypothesised two thrust planes (Fig. 5 of Merlino et al., 2000). Indeed active tectonic deformation on the margin has generated a suite of vertical offsets that have affected superficial deposits, particularly along the western sector, whereas the Apulian swell dipped down into the Taranto trench (Fig. 8) through several westward-dipping deep-seated faults (Fusi et al., 2006). The eastern limbs of the large-scale narrow ridges (related to the western tilted and faulted blocks that dissect the Apulian antiform) showed a gentler slope, while to the west the flanks were steeper and the associated chirp echo-type suggests predominant erosion (echo-type L₁). Their axes occurred parallel to NWN–SES fault scarps, plunging westward with hard substrata outcropping at their tops. Here extensive erosion has been documented (Malinverno et al., 2010). Such a configuration has been inferred (Fusi et al., 2006) as being a system of superficial anticlinal folds and faults, interpreted as minor tensional and ductile compressive structures, connected with the hinge zone of the Apulian lithospheric anticline. These features suggest that tectonic deformation has continued to occur in recent times, even if the interpretation of the kinematics of these tectonic features remains controversial (Merlino et al., 2000; Argnani et al., 2001).

Evidence from sediment samples (Malinverno et al., 2010), coupled with observations from seismic data (Fig. 8), speaks to the presence of widespread erosion on the western side of the ridges, which has led to the emergence of stiff and/or hardened substrata, constituted by older sediments. Such outcropping hard beds represent a possible suitable substratum for coral growth.

5.4. CWC relation to morphologies: the broad mass-wasting area

The different surface expression of mass-transport deposits and related small-scale geomorphic features presented us with an opportunity to understand their relation with the CWC distribution.

According to Coleman and Prior (1988) and based on identified failure-related morphologies (Figs. 11, 12, 14 and 15), we have interpreted the dominant blocky pattern affecting the failed deposits as being related to slide events where slabs of soft sediment or partially lithified sediments were displaced in a downslope direction. The identified geometries shaping the blocky pattern area (i.e. the spatial relationship between the blocks of sediment, the recognition of compressional and extensional features, the identified downslope trending lineations, etc.) were not homogeneous over the whole area influenced by mass-transport deposits. This observation suggests that sediments experienced distinct transport along the whole slope due to different mechanisms of failure dynamics and different failure events that affected the upper slope.

Within the central and eastern broad mass-wasting area, the CWCs occurred as developed reefs (Vertino et al., 2010) on clustered (and isolated) mound-like features. As resolved by side-scan sonar backscattering images, supported by video ground truthing, a dense coverage of (live and dead-fossil) coral frameworks ca 0.5–1 m high (Vertino et al., 2010) occurred on the top as well as along the northeastern flanks of such small-scale positive reliefs (Fig. 10). A limited number of cores were taken on exposed

slide deposits associated with CWC occurrences, one of which was collected hemipelagic silts containing coral fragments in its upper sequence. The underneath part consisted almost entirely of a stiff mud and lithogenic silt with folded strata, resembling failed deformed sediments, dating back to the late Pleistocene (Malinverno et al., 2010). The same core data documented a coral colonization dating back at least to the Younger Dryas (Malinverno et al., 2010). The observation suggests no later than a late Pleistocene time of deposition for such a failure, which occurred, in all likelihood, before the coral colonization and therefore before or during the Last Glacial Maximum (LGM). The failure exposure occurred were, as suggested by hydrologic models (Budillon et al., 2010; Manca et al., 2002) and current measurements (Kovacevic et al., 1999), enhanced along-slope bottom currents (coming from NE) were present and likely prevented the burial of mass-transport deposits.

CWC are mainly found where high transparent hyperbolics occur within facies III-1 and III-2. Such hyperbolics (where the CWC occurrence has been documented by video observation and sampling results) were characterised by higher elevations relative to the surrounding sediments. The latter consideration may suggest that the resulting morphologic pattern of CWC occurrences reflects the interaction between:

- (a) the complex small-scale irregular topography created by failure events, which likely exposed older strata at the seafloor, creating the necessary substrates for coral colonization along small-scale topographic highs. Such highs could be failed blocks of sediments and/or extensional ridges that characterized the upper-central sector. Indeed extensional features are common within the upper areas of slides that are not fully evacuated (Masson et al., 1998);
- (b) coral growth, whose consequent sediment trapping during the time of accretion (Freiwald et al., 2004) enhanced their elevation with respect to the surrounding seafloor;
- (c) bottom currents, which prevented coral burial.

Such mass-wasting depositional bodies, where parabolic features occur possibly due to more coherent blocks of material within the disaggregated mass, seemed to offer the main preferred substrate to CWC colonization.

5.5. CWC relation to morphologies: evidence of bottom-current activity

Hemipelagic sedimentation in the form of prominent drift occurs along the central ridge. The geometry of forming reflectors resembles contourite deposits (Faugères et al., 1999), at least for the uppermost part of the sedimentary succession (Fig. 9). The drift deposit was bounded to the east by a sharp failure scar, and the related failed deposit was well depicted by collected seismic profiles, as the result of a slump event. Contourite deposits can be highly sensitive to failure due to their high sedimentation rate (Sultan et al., 2004), in particular when they are formed in the upper portion of the slope within a tectonically active area, as in the case of the Apulian swell. Due to these considerations, we interpreted the uppermost part of sedimentary succession in the central ridge as a drift deposit that failed eastward, along its depocenter. A broad field of sediment waves lies on the resulting deposit. As in the case of the Humboldt slide (Lee et al., 2002), such sediment waves may represent the resulting morphology of a slump event such as slump compression waves rather than current-related depositional features. However, considering the absence of internal reflectors, with the exception of a few and spread thin surface reflectors, the bottom-current flow direction

(Budillon et al., 2010) and their crest orientation, we cannot dismiss the distinct possibility of a bottom-current-related developments.

We have no direct measurements of bottom-current direction. Assuming that currents generally follow the bathymetric contours suggests that a bottom current coming from the NE may be accelerated by seafloor morphology, such as the NWN-SES-oriented structural wedge extruded upward along the Apulian swell, on which sediment drift formed (Fig. 9). Such a drift highlights the importance of ADW flow over the investigated area.

According to our interpretation of chirp-sonar echo-type IV_3 and evidence on the associated side-scan-sonar mosaic (Fig. 13), the western flank of the central ridge is affected by erosion and reworking, possibly due to debris-flow vs. turbiditic events. The result is a rough topography formed, which could be interpreted either as erosional remnants or as more consolidated blocks of sediments transported by gravity flows. The reliefs were not higher than 3 m, on which CWC were visually observed and sampled. The lack of CWC at the top of the drift and over its eastern failed deposit is ascribed to the absence of proper substrata for coral colonization, whereas the spatial occurrence of bottom-current-induced seafloor features documented the action of ADW flow on the seafloor. In addition, the prograding part of the sediment drift was subject to a high rate of sedimentation, which was not conducive for coral growth.

ADW outflow was recognised as a core of more oxygenated and dense water located between 500 and 1000 m (Budillon et al., 2010). Such a depth range was the same at which we also found (1) exposed mass-wasting deposits hosting well-developed CWC thickets on elevated reliefs; (2) debris-flow deposits emplaced on the western flank of the central ridge where the CWC were patchy and in small colonies; and (3) western regional anticlines, with hard substrata outcropping at their tops, where a brief visual observation found small-scale colonies of *Madrepora* (MS08 site in Fig. 10—Etiope et al., 2010; Malinverno et al., 2010). These observations allowed us to ascribe the crucial importance of ADW flow in CWC occurrence and distribution, where both proper substrata and current exposure allowed for coral colonization and growth.

6. Conclusions

The described seafloor morphology and the dominant sedimentary processes that were identified within the investigated area, and their consequent correlation to cold-water coral distributions, provided the following observations:

- Tectonic, mass wasting and slope gradients seemed to be the main controlling mechanisms shaping the regional seascape of the southern Apulian margin. Their interaction resulted in filling, on the eastern side, of down-dropped hanging-wall basins by mass gravity-driven deposits, since the dominance of mass gravity-driven flows were recognised as the prevalent sedimentary process along the investigated area. The footwalls experienced uplift, becoming sites of prevalent erosion, particularly along the western side, where anticlines documented active and recent tectonic deformations.
- The prominent mass-transport deposition to the east and in the central area occurred both buried and exposed at the seafloor, associated with a variety of failure-related seafloor morphologies; unfortunately, the configuration made it difficult to discern single failure events.
- CWCs were mainly found along a depth belt between 500 and 900 m (1) within the most prominent mass-movements and

mass-transport deposition areas, (2) on debris deposits along the western flank of the central ridge, and (3) on hard substrata outcropping at the top of the anticlines that characterise the western part of the investigated area.

- The mass-transport deposit exposure occurred between 500 and 900, and the CWC were prevalently distributed along the top of the fault scarps. Their growth tended to enhance complex morphologies of the seabed, which appeared to have formed by clustered small-scale reliefs (coral mounds formed on failure-related seafloor morphologies?), whereas isolated mound-like morphologies, hosting coral frameworks, occurred mainly within the depressed areas.
- Drift sedimentation along the central ridge could document the importance of ADW flow on the investigated area, in the form of enhanced bottom currents which were able to prevent corals from burial, as the core of the ADW is located between 500 and 1000 m (Budillon et al., 2010) and mass-transport deposit exposure (where corals grow) occurs at this same depth range.

Acknowledgments

This study benefited from funding and ship-time through the FIRB 'Aplabes' program. We are grateful to Captains, Crew and Colleagues onboard RV *Universitatis* during APLABES cruises (2003–2005) and in particular to Chiara Tassarolo, Francesca Brega, Elisa Malinverno and Matthias Lopez-Correa for their support during the acquisition of the geophysical data. We also thank Colleagues onboard R/V *Urania* for the CNR cruises CORAL (2002), GECO (2005), and CORSARO (2006) during which useful discussion about cold-water coral helped to improve the manuscript. Special thanks are due to Marco Taviani and André Freiwald for fruitful scientific discussions, which contributed to improve the interpretation of the data here presented.

References

- Argnani, A., Favali, P., Frugoni, F., Gasperini, M., Ligi, M., Marani, M., Mattiotti, G., Mele, G., 1993. Foreland deformational pattern in the southern Adriatic Sea. *Annali di Geofisica* 36, 229–247.
- Argnani, A., Frugoni, F., Cosi, R., Ligi, M., Favali, P., 2001. Tectonics and seismicity of the Apulian Ridge south of Salento peninsula Southern Italy. *Annali di Geofisica* 44 (3), 527–540.
- Auroux, C., Mascle, J., Campredon, R., Mascle, G., Rossi, S., 1985. Cadre géodynamique et évolution récente de la Dorsale Apulienne et de ses bordures. *Giornale di Geologia* 3, 47 (1/2), 101–127.
- Billi, A., Salvini, F., 2003. Development of systematic joints in response to flexure-related fibre stress in flexed foreland plates: the Apulian forebulge case history. *Journal of Geodynamics* 36, 523–536.
- Billi, A., Salvini, F., 2000. Sistemi di fratture associati a faglie in rocce carbonatiche: nuovi dati sull'evoluzione tettonica del Promontorio del Gargano. *Bollettino della Società Geologica Italiana* 119, 237–250.
- Billi, A., Salvini, F., 2001. Fault-related solution cleavage in exposed carbonate reservoir rocks in the southern Apennines, Italy. *Journal of Petroleum Geology* 24, 147–169.
- Bosellini, A., Morsilli, M., Neri, C., 1999. Long-term event stratigraphy of the Apulia Platform Margin Upper Jurassic to Eocene, Gargano, Southern Italy. *Journal of Sedimentary Research* 69, 1241–1252.
- Budillon, G., Lo Bue, N., Siena, S., Spezie, G., 2010. Hydrographic characteristics of water masses and circulation in the northern Ionian Sea. *Deep-Sea Research II* 57 (5–6), 441–457.
- Boldrin, A., Miserocchi, S., Rabitti, S., Turchetto, M.M., Balboni, V., Socal, G., 2002. Particulate matter and circulation in the southern Adriatic and Ionian Sea: characterisation and downward fluxes. *Journal of Marine Systems* 33–34, 389–410.
- Calcagnile, G., Panza, G.F., 1981. The main characteristics of the lithosphere–asthenosphere system in Italy and surrounding regions. *Pure and Applied Geophysics* 119, 865–879.
- Camassi, R., Stucchi, M., 1996. NT4.1, un catalogo parametrico di terremoti di area italiana al di sopra della soglia del danno, <<http://emidius.itim.mi.cnr.it/NT/CONSNT.html>>.
- Coleman, J.M., Prior, D.B., 1988. Mass wasting on continental margin. *Annual Review of Earth and Planetary Sciences* 16, 101–119.
- Corselli, C., 2001. Change and Diversity: the Mediterranean Deep Corals from Miocene to the Present. *Mediterranean Ecosystem: Structures and Processes*. Springer-Verlag, Italia, pp. 361–366 (Chapter 7).
- Corselli, C., Favali, P., Rosso, M. A., Spezie, G., Taviani, M., Savini, A., Etiope, G., Tursi, A., Mastrototaro, F., Remia, A., APLABES CONSORTIUM, 2006. The Santa Maria di Leuca Lophelia reefs of the Mediterranean Sea: a research in progress. EGU General Assembly, Vien, 02–07 April 2006.
- Cushman-Roisin, B., Gacic, M., Poulain, P.M., Artegiani, A., 2001. In: Cushman-Roisin, K., et al. (Eds.), *Physical Oceanography of the Adriatic Sea Past, Present and Future*, p. 304.
- Damuth, J.E., 1980. Use of high frequency (3.5–12 kHz) echograms in the study of near bottom sedimentation processes in the deep sea. *Marine Geology* 38, 51–75.
- Damuth, J.E., Hays, D.E., 1977. Echo Character of East Brazilian Continental-Margin and Its Relationship to Sedimentary Processes. *Marine Geology* 24 (2), 73–95.
- D'Argenio, B., 1974. Le piattaforme carbonatiche periadriatiche. Una rassegna di problemi nel quadro geodinamico mesozoico dell'area mediterranea. *Memorie della Società Geologica Italiana* 13, 137–159.
- De Lazzari, A., Boldrin, A., Rabitti, S., Turchetto, M.M., 1999. Variability and downward fluxes of particulate matter in the Otranto Strait area. *Journal of Marine Systems* 20, 399–413.
- De Mol, B., Taviani, M., Canals, M., Remia, A., Alvarez, G., Busquets, P., Teixido, N., Gilli, J.M., 2005. Environmental and spatial distribution of Mediterranean cold-water corals. In: *Proceedings of the Third International Symposium on Deep-water Corals*, Miami, FL, p. 179.
- De Mol, B., Kozachenko, M., Wheeler, A., Alvares, H., Henriot, J.P., Olu-Le Roy, K., 2007. Thérèse Mound: a case study of coral bank development in the Belgica Mound Province, Porcupine Seabight. *International Journal of Earth Sciences* 96, 103–120.
- Dogliotti, C., Mongelli, F., Pieri, P., 1994. The Puglia uplift SE Italy: an anomaly in the foreland of the Apenninic subduction due to buckling of a thick continental lithosphere. *Tectonics* 13 (5), 1309–1321.
- Dorschel, B., Hebbeln, T.D., Rüggeberg, A., Dullo, W.C., Freiwald, A., 2005. Growth and erosion of a cold-water coral covered carbonate mound in the Northeast Atlantic during the Late Pleistocene and Holocene. *Earth and Planetary Science Letters* 233, 33–44.
- Etiope, G., Savini, A., Lo Bue, N., Favali, P., Corselli, C., 2010. Deep sea survey for the detection of methane at the "Santa Maria di Leuca" cold-water coral mounds Ionian Sea, South Italy. *Deep-Sea Research II* 57 (5–6), 431–440.
- Faugères, J.-C., Stow, D.A.V., Imbert, P., Viana, A., 1999. Seismic features diagnostic of contourite drifts. *Marine Geology* 162, 1–38.
- Favali, P., Funicello, R., Mattiotti, G., Mele, G., Salvini, F., 1993. An active margin across the Adriatic Sea central Mediterranean Sea. *Tectonophysics* 219, 109–117.
- Foubert, A., Depreiter, D., Beck, T., Maignien, L., Pannemans, B., Frank, N., Blamart, D., Henriot, J.-P., 2008. Carbonate mounds in a mud volcano province off north-west Morocco: key to processes and controls. *Marine Geology* 248, 74–96.
- Freiwald, A., 2002. Reef-forming cold-water corals. In: Wefer, G., Billelt, D., Hebbeln, D., Jørgensen, B.B., Schlüter, M., Van Weering, T. (Eds.), *Ocean Margin Systems*. Springer Verlag, Berlin, Heidelberg, pp. 365–385.
- Freiwald, A., Fossa, J.H., Grehan, A., Koslow, T., Roberts, J.M., 2004. Cold-water Coral Reefs—Out of Sight No Longer Out of Mind, UK UNEP-WCMC Biodiversity Series No. 22. UNEP-WCMC, Cambridge, pp. 1–88.
- Freiwald, A., Shipboard Party, 2007. Coral ecosystems in the central Mediterranean Sea. Meteor Cruise Reports, Hamburg.
- Freiwald, A., Beuck, L., Rüggeberg, A., Taviani, M., Hebbeln, D., 2009. The white coral community in the central Mediterranean Sea revealed by ROV surveys. *Oceanography* 22 (1), 58–74.
- Fusi, N., Savini, A., Corselli, C., 2006. High resolution (chirp) survey in the Ionian Sea (Italy, central Mediterranean): seismic evidence of mud diapirism and coral mounds. *Annals of Geophysics* 49 (2/3), 751–765.
- Gueguen, E., Dogliotti, C., Fernandez, M., 1998. On the post-25 Ma geodynamic evolution of the western Mediterranean. *Tectonophysics* 298, 259–269.
- Henriet, J.P., Kano, A., Malone, M.J., the Expedition 307 Project Team, 2005. Modern carbonate mounds: porcupine drilling. IODP Scientific Prospectus 307, <<http://iodp.tamu.edu/publications/SP/307SP/307SP.PDF>>.
- Hovland, M., Thomsen, E., 1997. Cold-water corals—Are they hydrocarbon seep related?. *Marine Geology* 137, 159–164.
- Huvenne, V.A.I., Beyer, A., De Haas, H., Dekindt, K., Henriot, J.P., Kozachenko, M., Olu-Le Roy, K., Wheeler, A.J., TOBI/Pelagia, 197 CARACOLE cruise participants, 2005. The seabed appearance of different coral bank provinces in the Porcupine Seabight, NE Atlantic: results from sidescan sonar and ROV seabed mapping. In: Freiwald, A., Roberts J.M. (eds.) *Cold-Water Corals and Ecosystems*. Springer, Berlin, Heidelberg, New York, pp. 535–569.
- Kenyon, N.H., Akhmetzhanov, A.M., Wheeler, A.J., van Weering, T.C.E., de Haas, H., Ivanov, M.K., 2003. Giant carbonate mud mounds in the southern Rockall Trough. *Marine Geology* 195, 5–30.
- Kovacevic, V., Gacic, M., Poulain, P., 1999. Eulerian current measurements in the Strait of Otranto and in the Southern Adriatic. *Journal of Marine Systems* 20, 255–278.
- Lee, H.J., Syvitski, J.P.M., Parker, G., Orange, D., Locat, J., Hutton, E.W.H., Imran, J., 2002. Distinguishing sediment waves from slope failure deposits: field examples, including the 'Humboldt slide' and modelling results. *Marine Geology* 192 (1–3), 79–104.

- Malanotte-Rizzoli, P., Manca, B., Ribera d'Alcala, M., Theocharis, A., Bergamasco, A., Bregant, D., Budillon, G., Civitaresse, G., Georgopoulos, D., Michelato, A., Sansone, E., Scarazzato, P., Souvermezoglou, E., 1997. A synthesis of the Ionian Sea hydrography, circulation and water mass pathways during POEM Phase I. *Progress in Oceanography* 39, 153–204.
- Malinverno, A., Ryan, W.B.F., 1986. Extension of the Tyrrhenian Sea and shortening in the Apennines as result of arc migration driven by sinking lithosphere. *Tectonics* 5, 227–245.
- Malinverno, E., Taviani, M., Rosso, A., Violanti, D., Villa, I., Savini, A., Vertino, A., Remia, A., Corselli, C., 2010. Stratigraphic framework of the Apulian deep-water coral province, Ionian Sea. *Deep-Sea Research II* 57 (5–6), 345–359.
- Manca, B.B., Kovacevic, V., Gacic, M., Viezzoli, D., 2002. Dense water formation in the Southern Adriatic Sea and interaction with the Ionian Sea in the period 1997–1999. *Journal of Marine Systems* 33–34, 133–154.
- Manca, B.B., Ibello, V., Pacciaroni, M., Scarazzato, P., Giorgetti, A., 2006. Ventilation of deep waters in the Adriatic and Ionian Sea following changes in thermohaline circulation of the Eastern Mediterranean. *Climate Research* 31, 239–256.
- Mantziafou, A., Lascaratos, A., 2004. An eddy resolving numerical study of the general circulation and deep-water formation in the Adriatic Sea. *Deep-Sea Research I* 51, 921–952.
- Marani, M., Argnani, A., Roveri, M., Trincardi, F., 1993. Sediment drifts and erosional surfaces in the central Mediterranean: seismic evidence of bottom-current activity. *Sedimentary Geology* 82, 207–220.
- Masson, D.G., Canals, M., Alonso, B., Urgeles, R., Hqnerbach, V., 1998. The canary debris flow: source area morphology and failure mechanisms. *Sedimentology* 45, 411–432.
- Mastrototaro, F., D'Onghia, G., Corriero, G., Matarrese, A., Maiorano, P., Panetta, P., Gherardi, M., Longo, C., Rosso, A., Sciuto, F., Sanfilippo, R., Gravili, C., Boero, F., Taviani, M., Tursi, A., 2010. Biodiversity of the white coral bank off Cape Santa Maria di Leuca (Mediterranean Sea): An update. *Deep Sea Research II* 57 (5–6), 412–430.
- Merlini, S., Cantarella, G., Doglioni, C., 2000. On the seismic profile Crop M5 in the Ionian Sea. *Bollettino della Societa' Geologica Italiana* 119, 227–236.
- Minisini, D., Trincardi, F., Asioli, A., 2006. Evidence of slope instability in the southwestern Adriatic margin. *Natural Hazards and Earth System Sciences* 6 (1), 1–20.
- Moretti, I., Royden, L., 1988. Deflection, gravity anomalies and tectonics of doubly subducted continental lithosphere: Adriatic and Ionian Seas. *Tectonics* 7, 875–893.
- Mortensen, P.B., Buhl-Mortensen, L., Gebruk, A.V., Kryolova, E.M., 2008. Occurrence of deep-water corals on the Mid-Atlantic Ridge based on MAR-ECO data. *Deep-Sea Research II* 55, 142–152.
- Prior, D.B., Bornhold, B.D., Coleman, J.M., Bryant, W.R., 1982. Morphology of a submarine slide, Kitimat Arm, British Columbia. *Geology* 10, 558–592.
- Rebesco, M., Larter, R.D., Camerlenghi, A., Barker, P.F., 1996. Giant sediment drifts on the continental rise west of the Antarctic Peninsula. *Geo-Marine Letters* 16, 65–75.
- Ricchetti, G., Ciaranfi, N., Luperto Siani, E., Mongelli, F., Pieri, P., 1988. Geodinamica ed evoluzione sedimentaria e tettonica dell'avampaese apulo. *Memorie della Societa' Geologica Italiana* 41, 57–82.
- Ridente, D., Trincardi, F., 2006. Propagation of shallow folds and faults in late Pleistocene and Holocene shelf-slope deposits, central and South Adriatic Margin (Italy). *Basic Research* 18, 171–188.
- Roberts, J., Wheeler, A.J., Freiwald, A., 2006. Reefs of the Deep: the biology and geology of cold-water coral ecosystems. *Science* 312, 543–547.
- Roberts, J. M., Wheeler, A. J., Freiwald A., Cairns, S., 2009. *The Biology and Geology of Deep-sea Coral Habitats*. Cambridge University Press.
- Robinson, A.R., Malanotte-Rizzoli, P., Hecht, A., Michelato, A., Roether, W., Theocharis, A., Ünlüata, Ü., Pinardi, N., Artegiani, A., Bergamasco, A., Bishop, J., Brenner, S., Christianidis, S., Gacic, M., Georgopoulos, D., Golnaraghi, M., Hausmann, M., Junghaus, H.G., Lascaratos, A., Latif, M.A., Leslie, W.G., Lozano, C.J., Oguz, T., Özsoy, E., Papageorgiou, E., Paschini, E., Rozentroub, Z., Sansone, E., Scarazzato, P., Schlitzer, R., Spezie, G.C., Tziperman, E., Zodiatis, G., Athanassiadou, M., Gerges, M., Osman, M., 1992. General circulation of the Eastern Mediterranean. *Earth-Science Review* 32, 285–309.
- Rosso, A., Vertino, A., Di Geronimo, I., Sanfilippo, R., Sciuto, F., Di Geronimo, I., Violanti, D., Taviani, M., Tursi, A., Mastrototaro, F., 2010. Hard versus soft-bottom thanatofacies from the Santa Maria di Leuca deep-water coral mound province, Recent Mediterranean. *Deep-Sea Research II* 57 (5–6), 360–379.
- Sager, W.W., Lee, C.S., MacDonald, I.R., Schroeder, W.W., 1999. High-frequency near-bottom acoustic reflection signatures of hydrocarbon seeps on the Northern Gulf of Mexico continental slope. *Geo-Marine Letter* 18 (4), 267–276.
- Salvini, F., Billi, A., Wise, D.U., 1999. Strike-slip fault-propagation cleavage in carbonate rocks: the Mattinata Fault Zone, Southern Apennines, Italy. *Journal of Structural Geology* (21), 1731–1749.
- Sánchez, F., Serrano, A., Parra, S., Ballesteros, M., Cartes, J.E., 2008. Habitat characteristics as determinant of the structure and spatial distribution of epibenthic and demersal communities of Le Danois Bank (Cantabrian Sea, N. Spain). *Journal of Marine Systems* 72, 64–86.
- Savini, A., Lo Bue, N., Malinverno, E., Corselli, C., Di Geronimo, I., Rosso, A., Tursi, A., 2004. Carbonate mounds on the Apulian continental slope: morphology, distribution and their relation with dead and living deep water corals. In: 23rd National Congress GNGTS, Rome, pp. 371–374.
- Schroder-Ritzrau, A., Mangini, A., Lomitschka, M., 2003. Deep-sea corals evidence periodic reduced ventilation in the North Atlantic during the LGM/Holocene transition. *EPSL* (216), 399–410.
- Schembri, P.J., Dimech, M., Camilleri, M., Page, R., 2007. Living deep-water *Lophelia* and *Madrepora* corals in Maltese waters (Strait of Sicily, Mediterranean Sea). *Cahiers de Biologie Marine* 48, 77–83.
- Taviani, M., Remia, A., Corselli, C., Freiwald, A., Malinverno, E., Mastrototaro, F., Savini, A., Tursi, A., 2005a. First geo-marine survey of living cold-water *Lophelia* reefs in the Ionian Sea (Mediterranean Basin). *Facies* (50), 409–417.
- Taviani, M., Freiwald, A., Zibrowius, H., 2005b. Deep coral growth in the Mediterranean Sea: an overview. In: Freiwald, A., Roberts, J.M. (Eds.), *Cold-Water Corals and Ecosystems*. Springer, Berlin, Heidelberg, New York, pp. 137–156.
- Tramutoli, M., Pescatore, T., Senatore, M.R., Mirabile, L., 1984. Interpretation of reflection high resolution seismic profiles through the Gulf of Taranto (Ionian Sea, Eastern Mediterranean). The structure of Apennine and Apulia deposits. *Bollettino di Oceanologia Teorica ed Applicata* 2, 33–52.
- Trincardi, F., Fogliani, F., Verdicchio, G., Asioli, A., Correggiari, A., Minisini, D., Piva, A., Remia, A., Ridente, D., Taviani, A., 2007. The impact of cascading currents on the Bari Canyon System, SW-Adriatic Margin (Central Mediterranean). *Marine Geology* 246, 208–230.
- Tursi, A., Mastrototaro, F., Matarrese, A., Maiorano, P., D'Onghia, G., 2004. Biodiversity of the white coral reefs in the Ionian Sea (Central Mediterranean). *Chemistry and Ecology* 20 (1), 107–116.
- Vertino, A., Savini, A., Rosso, A., Di Geronimo, I., Mastrototaro, F., Sanfilippo, R., Gay, G., Etiope, G., 2010. Benthic habitat characterization and distribution from two representative sites of the deep-water SML Coral Mound Province (Mediterranean). *Deep-Sea Research II* 57 (5–6), 380–396.
- Wheeler, A.J., Beyer, A., Freiwald, A., de Haas, H., Huvenne, V.A.I., Kozachenko, M., Olu-Le Roy, K., Operbecke, J., 2007. Morphology and environment of cold-water coral carbonate mounds on the NW European margin. *International Journal of Earth Sciences* 96, 37–56.
- Williams, T., Kano, A., Ferdelman, T.G., Henriot, J.P., Abe, K., Andres, M.S., Bjaerager, M., Browning, E.L., Cragg, B.A., De Mol, B., Dorschel, B., Foubert, A., Frank, T.D., Fuwa, Y., Gaillot, P., Gharib, J.J., Greg, J.M., Huvenne, V.A.I., Léonide, P., Li, X., Mangelsdorf, K., Tanaka, A., Monteys, X., Novosel, I., Sakai, S., Samarkin, V.A., Sasaki, K., Spivack, A.J., Takashima, C., Titschack, J., 2006. Cold-water coral mounds revealed. *EOS, Transactions of the American Geophysical Union* 87 (47), 535–536 525.
- White, M., Roberts, J.M., van Weering, T., 2007. Do bottom-intensified diurnal tidal currents shape the alignment of carbonate mounds in the NE Atlantic? *Geo-Marine Letters* 27(6), 391–397.